ELECTRONICALLY DIABATIC PHOTODESORPTION OF MOLECULES ADSORBED ON METAL SURFACES

By

DARIO BEKŠIĆ

A DISSERTATION PRESENTED TO THE GRADUATE SCHOOL
OF THE UNIVERSITY OF FLORIDA IN PARTIAL FULFILLMENT
OF THE REQUIREMENTS FOR THE DEGREE OF
DOCTOR OF PHILOSOPHY

UNIVERSITY OF FLORIDA

1994

To Neus
to the memory of my mother
and to my dad

ACKNOWLEDGMENTS

First of all, I wish to thank my mom and dad for all the love, caring and wisdom that I was fortunate to receive throughout my life

I also want to acknowledge the merits of all my teachers at the University of Zagreb and the "Ruger Bošković Institute" for the good foundations in my profession, and especially thank Dr Nenad Trinajstić whose help was crucial for my arrival to the QTP

My most sincere thanks must go to David Micha for the wisdom of his advice, his seemingly infinite patience, and his human understanding, as well as to Mrs Becky for all those lovely reunions at their home It was a true pleasure to work and share good times with my group colleagues Keith (special thanks for his help with all my computer bugs, and for all good times at the basketball court) Herbert (special thanks for his friendship and patience) Robert, Joel, Eric, Jorge, Pierre and Zhigang, and our visitors Pepé, Salvador, Marcelo, Darío (the other one) and Gerardo I will fondly remember my friends in and out of the QTP: Henk Monkhorst and Mrs Alka, Joaquim (another special thanks for his friendship and kindness) Nata and Manel, Sonja and Hrvoje, and several others. They have made these five long years enjoyable after all

And last, but most certainly not least I wish to most cordially thank my wife Neus for her most wonderful love and beauty, for every one of our moments and especially for her understanding and patience to wait for them during the times of separation and longing, and my stepson Alma for his support for both of us and his good spirit

TABLE OF CONTENTS

ACKNOWLEDGMENTS iii

ABSTRACT vii

CHAPTERS

1 INTRODUCTION 1

- Statement of the Problem 1
- Previous Work on Diatomics Adsorbed on Metal Surfaces 2
- Outline for the Study of Photodesorption of CO from Ni(001) Surface 4

2. A PHYSICAL MODEL FOR PHOTODESORPTION OF CARBON MONOXIDE FROM TRANSITION METAL SURFACES 8

- Qualitative Description of the Ni(001)(ads)CO System 8
- Partitioning of an Extended Molecular System Within a Self-consistent Field Formulation 15
- Self-consistent Field Treatment of Energy Fluctuation and Dissipation 19
- Time Correlation Functions and their SCF Treatment 24
- Photodesorption Lifetime and Lineshape in terms of the TCFs 28

3 DYNAMICS OF THE SECONDARY DEGREES OF FREEDOM 32

- Classification of Secondary DF Excitations 32
- Quantum Dynamics of the Secondary Degrees of Freedom Phonons 33
- Quantum Dynamics of the Secondary Degrees of Freedom Electronic Excitations 38
- Form of the Primary-Secondary DF Coupling Hamiltonian 41
- Form of the Primary DF Energy Dissipation Operator 46

4 TIME EVOLUTION OF THE PRIMARY DEGREES OF FREEDOM 51

- TD Schrodinger Equation for the Primary DFs 51
- Electronic Representations 54
- Time Evolution Operator with the Split Operator Scheme 57

5 POTENTIAL ENERGY FUNCTIONS AND THEIR COUPLING FOR PRIMARY DEGREES OF FREEDOM 60

Primary DF Potential Energy Surfaces and their Couplings 60

Transition Dipole Moment for CO Photodesorption 68

Electronic Structure Calculations of the Region of Primary DFs 68

6 NUMERICAL ASPECTS OF TIME PROPAGATION 73

Methods of Time Propagation of Wavepackets with Dissipation 73

Initial Conditions for Wavepacket Propagation 78

Initial Conditions for the Wavefunction 78

Initial Conditions for the Dipole Amplitude 80

Numerical Parameters for Time Propagation 81

Algorithm for the Numerical Time Propagation 83

7 RESULTS OF CALCULATIONS AND DISCUSSION 86

Model Calculations for Dissipative Potential Parameters 86

Calculations of CO Photodesorption Varying the Incident Light Wavelength 89

Calculations of CO Photodesorption Varying the Dissipation Strength 97

Calculations of CO Photodesorption Varying the Asymptotic Energy Difference between FESs 108

8 CONCLUSIONS 111

Contributions to the Theory of Photodesorption 111

Computational Algorithm for the CO Photodesorption from the Ni(001) Surface 113

Summary of Results of the CO Photodesorption Calculations 114

Outlook for Future Research 117

APPENDICES

A RATE CONSTANT IN TERMS OF A COLLISIONAL TIME CORRELATION FUNCTION FOR A DISSIPATIVE SYSTEM 119

B INPUT DATA FOR THE ZINDO CALCULATIONS OF NiCO and $Ni_{10}CO$ 123

C.FLOW CHART OF THE COMPUTER PROGRAM FOR TIME EVOLUTION OVER TWO COMPLEX PESs IN TWO DEGREES OF FREEDOM 125

BIBLIOGRAPHY 127

BIOGRAPHICAL SKETCH 136

Abstract of Dissertation Presented to the Graduate School
of the University of Florida in Partial Fulfillment of the
Requirements for the Degree of Doctor of Philosophy

ELECTRONICALLY DIABATIC PHOTODESORPTION OF MOLECULES ADSORBED ON METAL SURFACES

By

Dario Bekšić

December 1994

Chairman: David A. Micha
Major Department: Physics

Photodesorption of a molecule from a metal surface, following absorption of a visible or UV light, involves electronic transitions of the desorbing species coupled to the lattice vibrations and electron hole excitations of the substrate. This dissertation presents a general treatment of those phenomena, based on a stochastic theory of localized perturbations in an extended system. The treatment is later specialized for diatomic adsorbates, in particular carbon monoxide adsorbed on the (001) surface of nickel.

The extended molecular system Hamiltonian is divided into a term for the localized region of primary degrees of freedom (DFs) affected by the desorption coupled to the secondary DFs of the substrate that acts as a time evolving bath. A self-consistent treatment gives an effective Hamiltonian for the primary DFs that accounts for energy fluctuation and dissipation in terms of the properties of adsorbate and substrate. The assumption of Brownian motion in the substrate shows the physical origin of dissipation in the primary effective Hamiltonian in terms of time correlation functions (TCFs) of lattice displacements or electronic density fluctuations. A diabatic electronic representation is used to eliminate momentum couplings between adsorbate electronic states. The bath dynamics is studied for lattice vibrations and electronic excitations. To include interaction with light, a radiation field term and a system field coupling term are added to the Hamiltonian.

A time evolution algorithm is developed for a system with two DFs and two coupled complex potential energy surfaces (PESs) and applied to the CO(ads)Ni(001). The time dependent Schrödinger equation for the primary DFs is solved numerically, using time evolution of wavepackets. The primary DF wave function and the transition dipole amplitude are propagated over time to obtain the autocorrelation function and the dipole dipole TCF, respectively, physical initial conditions are specified and discussed for both cases. The lifetimes of desorbing species' quantum states are obtained from the autocorrelation functions, while a Fourier transform of the dipole TCF yields a generalized desorption lineshape for non-Hermitian dissipative Hamiltonians.

The primary PESs and their couplings were parametrized semiempirically using experimental data and the results of the INDO electronic structure calculations. Widths of the PESs and couplings, represented by imaginary potential functions, were estimated from the data on desorption lifetimes.

The results of the time propagation show that the energy dissipation to the substrate plays a crucial role in the dynamics of the desorbing species both at short times when it influences the transitions between the primary electronic states and at late times when it determines the photodesorption lifetime The desorption lineshape results show a peak positioned in qualitative agreement with a previous experimental result, there is also additional structure attributable to the internal vibrational excitations of the desorbing species

CHAPTER 1
INTRODUCTION

Statement of the Problem

Photodesorption of carbon monoxide from the nickel (001) surface is studied in this dissertation as an example of a broader class of problems including extended molecular systems interacting with light. These extended systems may be polyatomic molecules or molecules in solutions that interact strongly with the solvent; this work focuses on small (diatomic) molecules adsorbed on metal surfaces. The key idea of its approach is that the physical processes in the adsorbate-substrate complexes are localized, i.e. describable by a small number of coordinates or degrees of freedom (DFs) of the adsorbate molecule interacting with the metal substrate that contains a very large number of DFs describing different excitations in it. A physical model is developed, in which the desorption follows absorption of visible or UV light and is preceded by an electronic transition in the adsorbate-substrate complex, coupled to the lattice vibrations and electron-hole excitations of the substrate. One can thus introduce the concept of desorption induced by an electronic transition. The localized character of the molecule-metal interface processes makes it possible to classify the DFs in the system: those that describe the localized processes that lead to the desorption constitute the primary DFs of the system, and they are coupled to a very large number of secondary DFs of the substrate.

The aim of this study is to solve the time dependent Schrödinger equation (TDSE) for the adsorbate-substrate complex. The concept of primary and secondary DFs is used to partition the total Hamiltonian of the complex accordingly. It is then assumed that the primary and secondary DFs are coupled in a self consistent field (SCF) manner, and the total wavefunction of the system is written as a product of primary and secondary wavefunctions that depend upon the respective DFs only. This formulation gives separate TDSEs for the two sets of DFs and this work focuses on solving the primary TDSE with an effective Hamiltonian that incorporates the effects of the substrate. The substrate dynamics is modeled stochastically for different types of excitations without the explicit solution of the secondary TDSE; this treatment leads to energy dissipation in the primary DF dynamics that is included as a non-Hermitian part of the primary effective Hamiltonian. The primary TDSE is then solved by means of wavepacket propagation; the propagation algorithm was constructed to include the presence of two electronic states of the adsorbate-substrate complex, and the effects of dissipation.

Previous Work on Diatomics Adsorbed on Metal Surfaces

The theoretical and experimental study of desorption induced by electronic transitions (DIET) has been a topic of considerable interest in recent years, with several literature reviews available [Tolk et al., eds., 1983; Brenig and Menzel, eds., 1986; Stulen and Knotek, eds., 1988; Betz and Varga, eds., 1990; Burns et al., eds., 1993]. In particular, the stimulated desorption has been discussed in reviews of experimental work [Lin and Ertl 1987; King and Cavanagh 1989; Avouris and Walkup 1989]. Experimental results have been obtained in particular for CO adsorbed on Ni using the electron energy loss spectroscopy (EELS) and the ultraviolet photoelectron spectroscopy (UPS) [Blyholder 1974, Akimoto et al 1979, López-Sancho and Rubio 1981].

Recent experimental results using time resolved spectroscopy have probed the substrate dissipation phenomenon in more detail and provide new information about the role of metal phonon and electron-hole excitations in systems such as CO adsorbed on Cu [Prybyla et al. 1990, 1992, Cavanagh et al. 1993] and CO adsorbed on Pt [Germer et al. 1993 and 1994]. The most recent theoretical work [Newns et al. 1991, Head-Gordon and Tully, I and II 1992] deals with these time resolved experiments.

The basic mechanism of stimulated desorption has been known for some time under the name of the Menzel Gomer Redhead (MGR) model [Menzel and Gomer 1964, Redhead 1964]. This model, originally constructed for atoms adsorbed on surfaces, consists of two electronic states of the adsorbate-substrate complex: a ground state with a potential well and a repulsive excited state. Absorption of visible or UV light, or scattering of e.g. an electron beam, causes the electronic transition into the repulsive excited state and the system continues to evolve over time in it.

A similar, but more complicated desorption mechanism is the desorption induced by multiple electronic transitions (DIMET). It occurs when the excited electronic state is also a bound state, so the diatomic cannot directly desorb in it. Instead it deexcites back into the ground electronic state, but into a distribution of its internal (mostly vibrational) states. This process can be repeated several times if the electronic excitation is continuously induced e g by light pulses of visible or UV frequencies corresponding to the electronic excitation energies, until the diatomic eventually desorbs in its ground electronic state with some vibrational distribution Examples of this behaviour are NO adsorbed on Pt [Gadzuk et al 1990] and on Pd [Misewich et al 1992]

Notably the MGR model does not incorporate the continuum properties of the substrate, nor does it include in its original version the internal (vibrational and rotational) primary degrees of freedom In more recent theoretical studies the continuum of substrate excitations has been included as a finite width of the primary potential energy surfaces (PESs) The width is expressed as an imaginary potential in scattering theory [Micha 1976] Its form has been derived e g from the propagator theory [Brenig 1976] or more recently in theory of adsorbate spectroscopy [Cederbaum and Tarantelli 1993] It can be shown that the form of these imaginary potentials is directly related to the stochastic properties of the substrate dynamics [Bekšić and Micha, to be publ] The vibrational motion of diatomics adsorbed on surfaces has also been amply studied, in particular for CO adsorbed on Ni [Richardson and Bradshaw 1979 Black et al 1981 and 1982 Parra and Micha 1986 Micha and Parra 1988] on Cu [Persson and Persson I and II 1980 Head Gordon and Tully 1992] and on Pt [Persson and Ryberg 1989]

Outline for the Study of Photodesorption of CO from Ni(001) Surface

The rest of this dissertation focuses on the specific problem of carbon monoxide adsorbed on the Ni(001) surface

Chapter 2 contains the physical model for this extended system, based on earlier theoretical [Sung and Hoffmann 1985 Hoffmann 1988 Drakova and Doyen 1990] and experimental [Akimoto et al 1979, López Sancho and Rubio 1981] studies The localized character of the photodesorption motivates the concept of partition into the primary and the secondary region [Kumamoto and Silbey 1982, Miller 1987, Gerber and Ratner 1988 Micha and Srivastava 1989 Srivastava and Micha I and II 1991 Coalson 1989, Messina and Coalson 1991] and the effective Hamiltonians in terms of the degrees of freedom of both regions are derived within the self-consistent field treatment This treatment shows the connection between the energy dissipation in the secondary region as a continuum of surface states and the imaginary potentials introduced phenomenologically through scattering theory [Micha, 76] Time correlation functions are introduced at this point as well as their SCF formalism Physical properties such as lifetime of desorbing states and photodesorption lineshape are expressed in terms of the TCFs and the lineshape is derived for systems with energy dissipation The detailed derivation for a transition probability with a dissipative Hamiltonian related to the lineshape is presented in Appendix A

The stochastic dynamics of the secondary DFs is studied in detail in Chapter 3, for the cases of surface phonons and electron hole excitations The lattice vibrations are described through the time dependence of substrate normal mode coordinates and conjugate momenta while the electron-hole excitations are described by a time-dependent one-electron density operator In both cases the SCF coupling between primary and secondary DFs leads to a primary DF dissipative

Hamiltonian that depends upon the integrated time correlation function of the vibrational displacements or the electronic density fluctuations

The primary DF time evolution, governed by the corresponding time dependent Schrödinger equation, is described in Chapter 4 with adiabatic and diabatic representation for the primary DF electronic basis The treatment is then generalized to include interaction with light, defining the electron-field representation [Lin and George 1980] The primary time evolution operator is derived by using a modified split operator scheme [Feit Fleck and Steiger 1982] for the dissipative Hamiltonian

Chapter 5 presents a semiempirical parametrization of the primary DF complex potential energy surfaces (PESs) and the transition dipole moment The parametrization was obtained from the INDO electronic structure calculations [Ridley and Zerner 1973, Zerner et al 1980] for a CONi molecule and CO adsorbed on a Ni_{10} cluster The INDO Hartree Fock calculations gave as a result the ground state PES, which was then rescaled to fit the previously known theoretical [Drakova and Doyen 1990] and experimental [Heskett et al 1985] results The INDO CI calculations gave the excited states and the corresponding transition dipole moments the transition with the largest dipole moment gave the excited state PES for the Ni(001)(ads)CO system

Chapter 6 is a brief analysis of the computational aspects of this work. It is primarily concerned with the numerical time evolution of wavepackets [Feit Fleck and Steiger 1979 Leforestier et al 1991] it gives an outline of the computational algorithm used to generate results presented in this work and a comparison with other methods The flow diagram of the Fortran 77 program used can be found in Appendix B This chapter also contains a detailed discussion of the initial conditions for the propagation of both the primary nuclear wavefunction and the transition dipole amplitude, with the physical implications of the choices made

All numerical results of this study are presented in Chapter 7 they include properties such as expectation values of the primary DFs over time probabilities of finding the system in either electronic state the TCFs (autocorrelation and dipole TCF), the desorption lifetimes and lineshapes for several varied parameters in calculations. This work s results are compared with the previous ones and discussed in connection with the physical properties of the system studied leading to conclusions summarized in the final Chapter 8

CHAPTER 2
A PHYSICAL MODEL FOR PHOTODESORPTION OF CARBON MONOXIDE FROM TRANSITION METAL SURFACES

Qualitative Description of the Ni(001)(ads)CO System

The electronic structure of CO adsorbed on the transition metal surfaces and in particular the Ni(001) surface has been recently studied by several different approaches, such as density of states studies [Sung and Hoffmann 1985, Albert and Yates 1987] or studies of electronic charge transfer between the CO molecular orbitals and the Ni conduction band [Hoffmann 1988, Zangwill 1988] with experimental results coming from e.g. electronic energy loss spectroscopy [Akimoto et al. 1979]. Table 2.1 contains some relevant data on the Ni(001)(ads)CO system, shown in Fig. 2.1

All this work indicates the adsorption mechanism for CO proposed earlier [Hermann and Bagus 1977, Sung and Hoffmann 1985]: its highest occupied molecular orbital (HOMO) 5σ donates a fraction of its population into the electronic bands of nickel, and then the surface donates back a smaller fraction of its electronic population into the CO's lowest unoccupied molecular orbital (LUMO) 2π — thus a chemisorption bond is formed. As a consequence of the interaction with a quasicontinuum of Ni 3d–4s band states, the CO molecular orbitals split and broaden into two narrow bands each, such that the two bands coming from the 5σ CO orbital couple with the Ni 4p upper unoccupied band while the two bands coming from the 2π orbital couple with the 3d-4s conduction band This suggests that the basis set of electronic states in which the system is modeled must consist of modified MOs of CO — linear combinations of the CO HOMO and LUMO and the Ni conduction and upper empty band states A schematic electronic energy diagram for the Ni(001)(ads)CO showing the splitting and broadening of the CO molecular orbitals due to the interaction with the Ni surface, is given by Fig 2.2 To get a further insight of the system Fig. 2.3 presents a vibrational energy diagram [Parra and Micha 1986 Maruca et al 1990] for the Ni(001)(ads)CO illustrating the coupling of different oscillating modes for the adsorbate with the phonon bands of the substrate. Frequencies and symmetry characters of those modes are listed in table 2 II.

The density of states crystal orbital overlap population (COOP) results [Sung and Hoffmann 1985] show that the interaction between the carbon atom of CO and the adsorption site Ni atom is bonding in nature for the 5σ orbital while it is antibonding for the 2π orbital Those results suggest that the desorption of CO is induced by a transition from an occupied electronic band of the adsorbate substrate complex that is a combination of Ni $3d(x^2 - y^2)$ and Ni $3d(xy)$ bands into an empty band that is a mixture of Ni $4p(z)$ band and the carbon 2s atomic orbital which is antibonding between Ni and C

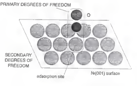

Figure 2.1 Sketch of the Ni(001)(ads)CO system

Table 2.1 Experimental data table for the Ni(001)(ads)CO system

Property	Magnitude	Reference
Ni conduction band (3d-4s) width	4 eV	Albert and Yates '87
Ni Fermi energy level	- 8.5 eV	Albert and Yates '87
Ni valence (3p) to conduction (3d-4s) band gap	> 45 eV	Bross et al '71
Ni conduction (3d-4s) to upper empty (4p) band gap	< 1 eV	Nagel '73
Ni upper empty band (4p) width	7 eV	Nagel '73
Ni Debye frequency	260 cm^{-1}	de Launay '55
CO binding energy	11 1 eV	Herzberg '60
CO equilibrium bond distance	2 132 bohr	Herzberg '60
C-Ni binding energy	1 3 eV	Heskett et al '85
C-Ni equilibrium distance	3 4 bohr	Andersson and Pendry '79
CO (5σ to 2π) excitation energy	8 6 eV	Akimoto et al '79

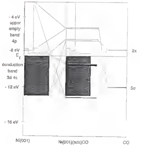

Figure 2.2 Qualitative electronic energy diagram for Ni(001)(ads)CO system

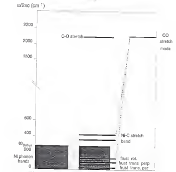

Figure 2.3 Vibrational energy diagram for Ni(001)(ads)CO system.

Table 2.II. Vibrational frequencies and symmetry characterizations for the normal modes of the Ni(001)(ads)CO system.

Description	Symmetry Character	Frequency (cm^{-1})	Reference
C-O stretch	A_1	2088 2069	Parra and Micha, 1986 Maruca et al., 1990
Ni C stretch	A_1	431 460	Parra and Micha, 1986 Maruca et al., 1990
NiCO frust. trans. (perp.)	A_1	102	Parra and Micha, 1986
NiCO bend	E	389	Parra and Micha, 1986
NiCO frust rot.	E	131	Parra and Micha, 1986
NiCO frust trans (parallel)	E	44	Parra and Micha, 1986

Since the Ni(001)(ads)CO is an extended system with a large number of degrees of freedom in the surface, it is virtually impossible to study exactly its quantum dynamics. However, numerous studies in which the Ni surface is substituted by a finite cluster of Ni atoms [Parra and Micha 1986, Drakova and Doyen 1990 with refs. therein] suggest that the interaction of CO with the surface is quite localized around the adsorption site.

Due to the localized interaction, it should be possible to treat the region around the adsorbate molecule separately from the rest of the surface, and eventually apply the exact quantum dynamics only to the corresponding degrees of freedom

(DFs) while using approximate methods to describe the substrate itself and its coupling to the region of adsorption. This concept for description of the extended molecular systems has been used before to study various processes [Kumamoto and Silbey 1982, Miller 1987, Gerber and Ratner 1988, Coalson 1989, Messina and Coalson 1991], such as photodissociation of extended molecules [Srivastava and Micha I and II 1991].

Partitioning of an Extended Molecular System Within a Self-consistent Field Formulation

An extended molecular system like a molecular adsorbate may be described by a Hamiltonian operator that is composed of three terms $\hat{H} = \hat{H}_S + \hat{H}_M + \hat{H}_{SM}$ corresponding to the Hamiltonians for the substrate surface, the adsorbate molecule, and their coupling. For a strongly coupled system, it is more convenient to instead write the Hamiltonian as a sum of terms relating to primary and secondary DFs, the primary and secondary Hamiltonian terms, and the coupling term, i.e.

$$\hat{H} = \hat{H}_p\left(\vec{X}, \frac{\partial}{\partial \vec{X}}\right) + \hat{H}_s\left(\left\{B\right\}\right) + \hat{H}_{ps}\left(\vec{X}, \frac{\partial}{\partial \vec{X}}, \left\{B\right\}\right) \qquad (2.1)$$

where $\vec{X}$ represents the set of primary DFs and $\{B\}$ stands for the collection of boson like operators B_j (and their adjoints $B_j^\dagger$) describing the collective excitations labelled by quantum numbers j which arise from interactions of the secondary DFs. In the case of diatomic adsorbates, the set $\vec{X}$ contains at least the diatomic bond distance r and the distance R from the center of mass of the diatomic to the surface. The collective modes of the substrate are phonons or electronic density fluctuations The time dependent Schrödinger equation (TDSE)

$$i\hbar\frac{\partial}{\partial t}|\Psi(t)\rangle = \hat{H}|\Psi(t)\rangle \tag{2.2}$$

where $\Psi(t)$ is the total wavefunction of the system must be solved for an initial value Ψ^0 at time $t = 0$. In an extended system, thermodynamical constraints and initial conditions lead to a distribution of the set of states $\{\Psi^0_\mu\}$ characterized by the statistical weights $\{w_\mu\}$ The mean value of a property $\hat{A}$ at time t is therefore given by

$$\langle\langle A(t)\rangle\rangle = \sum_\mu w_\mu \langle\Psi^0_\mu|\hat{A}(t)|\Psi^0_\mu\rangle \tag{2.3}$$

Two properties of particular relevance are the probability of survival of state μ at time t, following excitation by a light pulse obtained from $\hat{A} = |\Psi_\mu(t)\rangle\langle\Psi_\mu(t)|$ so that

$$P_\mu(t) = \frac{|\langle\Psi^0_\mu|\Psi_\mu(t)\rangle|^2}{\langle\Psi^0_\mu|\Psi^0_\mu\rangle\langle\Psi_\mu(t)|\Psi_\mu(t)\rangle} \tag{2.4}$$

and the lineshape for photodesorption by a steady light field, obtained in the dipole approximation from the Fourier transform of

$$L(t) = \sum_{\mu,\nu} w_\mu \frac{\langle\Psi^0_\mu|D(0)^\dagger D(t)|\Psi_\nu(t)\rangle}{\langle\Psi^0_\mu|\Psi^0_\mu\rangle\langle\Psi_\nu(t)|\Psi_\nu(t)\rangle} \tag{2.5}$$

where D is a transition dipole operator for light absorbed during desorption Depending on the wavelength of the absorbed light and on the nature of the system this transition dipole may depend on the adsorbate or the substrate DFs

The states $\Psi_j(t)$ must be obtained in an approximation suitable to localized phenomena in extended systems One such approximation is the self-consistent field (SCF) formulation in which the state is factored into primary and secondary DFs states ψ^p_α and ψ^s_β. This approximation is limited to short time events and is most accurate when used to calculate expectation values of additive properties. In this case, its validity may be expected to increase because statistical properties are being calculated, resulting from weighted sums over states and therefore showing less susceptibility to approximations to single states. One proceeds by first focusing on a single state for given quantum numbers $\mu=(\alpha,\beta)$ and later averaging over the states β.

In the self-consistent field (SCF) formulation of the problem, it is assumed that the total wavefunction of the system can be written as a product of the primary and secondary DFs wavefunctions with a phase factor, i.e.

$$|\Psi_\mu(t)\rangle = |\psi^p_\alpha(t)\rangle|\psi^s_\beta(t)\rangle\exp[i\chi(t)] \tag{2.6}$$

where each time dependent factor is a function of coordinates of the corresponding region only. These factors and the time-dependent phase χ satisfy differential equations derived with the time-dependent variational method [Micha and Srivastava 1989]. The TDSE splits into two SCF equations for the respective DFs of the system, omitting the state indices

$$i\hbar\frac{\partial}{\partial t}|\psi^p(t)\rangle = F_p(t)|\psi^p(t)\rangle \tag{2.7}$$

and

$$i\hbar\frac{\partial}{\partial t}|\psi^s(t)\rangle = F_s(t)|\psi^s(t)\rangle \tag{2.8}$$

The effective Hamiltonians are given by

$$\begin{gathered} F_p(t) = H_p + h_p(t) \\ h_p(t) = \langle\psi^s(t)|\hat{H}_{ps}|\psi^s(t)\rangle/\langle\psi^s(t)|\psi^s(t)\rangle \end{gathered} \tag{2.9}$$

and

$$\begin{aligned} F_s(t) &= H_s + h_s(t) \\ h_s(t) &= \langle\psi^p(t)|H_{ps}|\psi^p(t)\rangle / \langle\psi^p(t)|\psi^p(t)\rangle \end{aligned} \tag{2.10}$$

where the Dirac bracket notation in each case implies integration over the corresponding DFs.

A necessary condition for the validity of the SCF treatment is established by the nature of the operators that describe the physical process of interest; these operators must depend only upon the primary or secondary DFs, but not on both. The case where the operator depends on the primary DFs has been investigated for photodissociation with a similar formulation [Srivastava and Micha 1991]. In this case, the operators are transition dipoles for light absorption which can depend on the primary or secondary DFs.

The SCF calculations provide the time-evolution of the total state. If this is given by a wavepacket at the initial time, corresponding to the excitation conditions, the survival probability of a chosen state follows, omitting the state index μ, from

$$\begin{aligned} P(t) &= P^p(t)P^s(t) \\ P^p(t) &= \frac{|\langle\psi^p(0)|\psi^p(t)\rangle|^2}{\langle\psi^p(0)|\psi^p(0)\rangle\langle\psi^p(t)|\psi^p(t)\rangle} \\ P^s(t) &= \frac{|\langle\psi^s(0)|\psi^s(t)\rangle|^2}{\langle\psi^s(0)|\psi^s(0)\rangle\langle\psi^s(t)|\psi^s(t)\rangle} \end{aligned} \tag{2.11}$$

and the spectral lineshape for desorption is given, when the transition dipole depends only on the primary degrees of freedom, by

$$\begin{aligned} L(t) &= L^p(t)L^s(t) \\ L^p(t) &= \frac{\langle\psi^p(0)|D_p(0)^\dagger D_p(t)|\psi^p(t)\rangle}{\langle\psi^p(0)|\psi^p(0)\rangle\langle\psi^p(t)|\psi^p(t)\rangle} \\ L^s(t) &= \frac{\langle\psi^s(0)|\psi^s(t)\rangle}{\langle\psi^s(0)|\psi^s(0)\rangle\langle\psi^s(t)|\psi^s(t)\rangle} \end{aligned} \tag{2.12}$$

where $\hat{D}_p(t) = \exp\left(-i\hat{F}_p t/\hbar\right) D_p(0) \exp\left(i\hat{F}_p t/\hbar\right)$ is the transition dipole moment operator; it is a function of primary DFs and it will be discussed in more detail later. The primary effective Hamiltonian $\hat{F}_p(t)$ derived from the above formalism does not include interaction of the adsorbate substrate complex with light.

If it is necessary to describe the preparation of the initial adsorbate-substrate state by light absorption, then the total Hamiltonian of the system must be expanded [Louisell 1973] so that, for the primary DFs, it becomes

$$F_{pL} = \hat{F}_p + \hat{H}_L + H_{pL} = F_p + \sum_{\vec{k}} \omega_{\vec{k}} \hat{c}^{\dagger}_{\vec{k}} \hat{c}_{\vec{k}} - \vec{\mathcal{E}}(t) \cdot \vec{D}_p \tag{2.13}$$

where now $\hat{F}_p$ is the previously defined primary effective Hamiltonian, $\hat{H}_L$ is the Hamiltonian of the quantized radiation field in vacuo, and $\hat{H}_{pL}$ is their coupling. The quantized electric field in the Schrödinger picture is given by

$$\vec{\mathcal{E}} = i \sum_{\vec{k}} \sum_{\pi} \sqrt{\frac{\omega_{\vec{k}}}{2\epsilon_0}} \left[\hat{c}_{\vec{k}} - c^{\dagger}_{\vec{k}}\right] \vec{e}_{\pi} \tag{2.14}$$

where the index π denotes polarization. Operators $c^{\dagger}_{\vec{k}}$ and $\hat{c}_{\vec{k}}$ are creation and annihilation operators for photons.

Self-consistent Field Treatment of Energy Fluctuation and Dissipation

The TD Schrödinger equations for the two sets of DFs

$$i\hbar \frac{\partial}{\partial t} |\psi^p(t)\rangle = \left[\hat{H}_p + h_p(t)\right] |\psi^p(t)\rangle \tag{2.15}$$

and

$$i\hbar \frac{\partial}{\partial t} |\psi^s(t)\rangle = \left[\hat{H}_s + h_s(t)\right] |\psi^s(t)\rangle \tag{2.16}$$

must be solved simultaneously. Here, it is assumed that the state of the secondary DFs has been found, and proceed to find the effective Hamiltonian describing the dynamics of the primary DFs It is convenient to introduce the interaction picture which develops from the primary Hamiltonian,

$$|\psi^p(t)\rangle^{(I)} = \exp\left(\frac{i}{\hbar}\bar{H}_p t\right)|\psi^p(t)\rangle \tag{2.17}$$

This new wavefunction is then introduced into (2.17), which becomes

$$i\hbar\frac{\partial}{\partial t}|\psi^p(t)\rangle^{(I)} = \hat{h}_p^I(t)|\psi^p(t)\rangle^{(I)} \tag{2.18}$$

with

$$\hat{h}_p^I(t) = \exp\left(\frac{i}{\hbar}\bar{H}_p t\right)\hat{h}_p(t)\exp\left(-\frac{i}{\hbar}H_p t\right) \tag{2.19}$$

The equation (2.18) is then formally integrated over time and after transforming back into the Schrödinger picture, the primary wavefunction is given by

$$|\psi^p(t)\rangle = \exp\left(-\frac{i}{\hbar}H_p t\right)|\psi^p(0)\rangle - \frac{i}{\hbar}\int_0^t \exp\left(-\frac{i}{\hbar}\bar{H}_p t'\right)h_p(t')|\psi^p(t')\rangle dt' \tag{2.20}$$

The procedure is continued by taking the solution (2.20) and introducing it back into the last term on the right hand side of (2.18) The result is an integrodifferential equation for the primary wavefunction reminiscent of the generalized Langevin (GLE) expression

$$\begin{aligned} i\hbar\frac{\partial}{\partial t}|\psi^p(t)\rangle &= \bar{H}_p|\psi^p(t)\rangle + R_p(t)|\psi^p(0)\rangle - \\ &-\frac{i}{\hbar}\int_0^t M_p(t\ t')|\psi^p(t')\rangle dt' \end{aligned} \tag{2.21}$$

The first term on the right hand side refers to motions of the primary DFs in the absence of the secondary DFs The second term is the energy fluctuation term its form, by comparison contains the random or fluctuation operator

$$R_p(t) = \frac{\langle\psi^s(t)|H_{ps}|\psi^s(t)\rangle}{\langle\psi^s(t)|\psi^s(t)\rangle}\exp(-i\bar{H}_p t/\hbar) \tag{2.22}$$

Finally, the last term is the "energy dissipation" term with the "memory kernel" given by

$$\tilde{M}_p(t,t') = \frac{\langle\psi^s(t)|H_{ps}|\psi^s(t)\rangle}{\langle\psi^s(t)|\psi^s(t)\rangle}\exp[-i\tilde{H}_p(t-t')/\hbar]\frac{\langle\psi^s(t')|H_{ps}|\psi^s(t')\rangle}{\langle\psi^s(t')|\psi^s(t')\rangle} \quad (2.23)$$

It must be noted here that Eq (2.23) has a somewhat different structure than the GLE that would have been obtained by partitioning the wavefunction into primary and secondary terms via projection operators notably, the exponential time evolution operator in the "memory kernel" is that of the primary rather than the secondary DFs However, it is obvious that

$$M_p(t,t') = \hat{R}_p(t)\hat{R}_p^{\dagger}(t') \quad (2.24)$$

and that evaluating a statistical average of both sides of this equation over a distribution of the secondary states would lead to the familiar fluctuation dissipation relation [Berne 1971]

So far the primary integrodifferential equation is formally exact, but to further give its form it is necessary to specify the secondary state In the particular case of surface adsorption, the secondary DFs contain a collection of quasicontinuous excitations with characteristic frequencies ranging from zero to values comparable to the energy differences of the discrete molecular energy levels of the adsorbate Therefore, it is appropriate to calculate the average fluctuation and dissipation terms with the statistical density operator

$$\hat{\Gamma}_s(t) = \sum_{\beta} w_{\beta}^s|\psi_{\beta}^s(t)\rangle\langle\psi_{\beta}^s(t)| \quad (2.25)$$

where the w_{β}^s are statistical weights for the set of initial states $\{\psi_{\beta}^s(0)\}$ e.g Boltzmann factors for the temperatures of the substrate or nonequilibrium weights if the system has been prepared in a nonstationary distribution of states. The components of the secondary wavefunction in general evolve over time with all possible combinations of the mentioned frequencies. Consequently one can assume that the secondary DFs rapidly reach temporary equilibrium, from which they can respond to driving forces; this leads to fluctuations and dissipation around a temporary equilibrium which can be characterized by e.g. a time dependent temperature.

The expectation values

$$h_p^{(\beta)}(t) = \langle \psi_\beta^s(t) | \hat{H}_{ps} | \psi_\beta^s(t) \rangle / \langle \psi_\beta^s(t) | \psi_\beta^s(t) \rangle \tag{2.26}$$

are chaotic and rapidly varying functions of time. The weighted sums of these expectation values and of their products can be expected to show extensive cancellations, of the type described by models of stochastic phenomena [Kubo, Toda, and Hashitsume 1989; van Kampen 1981]. Therefore, it is assumed that

(i) the fluctuation force averages out to zero on the primary time scale, i.e.

$$\langle\langle R_p(t) \rangle\rangle = \sum_\beta w_\beta^s R_p^{(\beta)}(t) = 0 \tag{2.27}$$

(ii) the statistical average of the memory kernel describes both instantaneous and delayed dissipations leading to a temporary equilibrium; hence one writes, introducing the Dirac delta function, that

$$\langle\langle M(t,t') \rangle\rangle = \sum_\beta w_\beta^s R_p^{(\beta)}(t) R_p^{(\beta)}(t')^\dagger = \frac{\hbar}{2} \hat{W}_p(t) \delta(t-t') + N_p(t) \eta(t-t') \tag{2.28}$$

where $\hat{W}_p$ is an operator in the primary DFs only, describing instantaneous dissipation at each time, while N_p describes a remaining persistent dissipation component with a time delay given by a function η analytical in the variable $t - t'$. This expression is sufficiently general to include the dissipation mechanisms that are expected. The two operators to the right depend on time because temporary thermal equilibrium is allowed for. They would be independent of time if the equilibrium were stable.

Under the above assumptions, Eq. (2.23) becomes a time-dependent integrodifferential Schrödinger equation with Hermitian and anti-Hermitian potentials

$$i\hbar\frac{\partial}{\partial t}|\psi^{p}(t)\rangle = [\hat{H}_{p} - \frac{i}{2}W_{p}(t)]|\psi^{p}(t)\rangle - \frac{i}{\hbar}\hat{N}_{p}(t)\int_{t_0}^{t} dt'\,\eta(t-t')|\psi^{p}(t')\rangle \quad (2.29)$$

The primary Hamiltonian is the sum of the kinetic energy and potential energy operators in the primary electronic and nuclear DFs,

$$\hat{H}_{p} = \hat{K}_{p} + \hat{V}_{p} \quad (2.30)$$

while the random force and memory term must be derived from explicit expressions for the secondary region Hamiltonian and from the coupling between the regions.

A more detailed treatment of the secondary dynamics is presented in the next chapter, where the time dependence of the secondary states is discussed for two types of excitations: quantized lattice vibrations (phonons) and electronic excitations. Consequently, the secondary Hamiltonian can be expressed as a sum of three terms

$$H_{s} = H_{s}^{v} + H_{s}^{e} + H_{s}^{ev} \quad (2.31)$$

where the first term refers to the lattice vibrations, the second to the electronic excitations, and the third to their coupling. The coupling Hamiltonian can again be expressed as a sum of vibrational, electronic and mixed terms

$$H_{ps} = H_{ps}^{v} + H_{ps}^{e} + H_{ps}^{ev} \tag{2.32}$$

This in turn gives a sum of SCF potentials

$$\bar{h}_p = \bar{h}_p^{v} + \bar{h}_p^{e} + \bar{h}_p^{ev} \tag{2.33}$$

in the primary effective Hamiltonian

To specify the Hamiltonian in more detail, one needs to choose the coordinates of substrate and adsorbate atoms. Two different choices are obvious: the first one would be appropriate if the adsorbate were to remain always bound and would consist of the vibrational normal coordinates for the whole system; the second choice introduces the normal coordinates Q_μ of the metal without the adsorbate, and the Jacobi (center-of-mass) coordinates $\vec{X}$ for the adsorbate relative to the metal surface. In the present study of desorption, the second choice is more convenient because it is appropriate for the description of the asymptotic motion of the molecule.

Time Correlation Functions and their SCF Treatment

A time correlation function (TCF) is generally defined as a projection of some time dependent amplitude onto the value of that amplitude at some specified time. There exists an abundant theoretical work demonstrating the relation of the TCFs with certain physical properties of the studied systems, for example reaction rate constants in terms of either flux-flux TCFs [Miller 1974; Miller et al. 1983] or collisional TCFs [Micha 1979; Micha and Villallonga 1985], dissociation line shapes in terms of transition dipole TCFs [Micha 1981; Srivastava and Micha

1989] etc These relations are based on the conversion of the Fermi golden rule for the state to state reaction rate [Rodberg and Thaler 1967 Schiff 1969]

$$R_{m\to n} = \frac{1}{\hbar}\left|\langle m|T|n\rangle\right|^2 \delta(E_m - E_n) \qquad (2.34)$$

where, symbolically, $|m\rangle$ is the initial and $|n\rangle$ is the final state of the system, and $\hat{T}$ is the transition operator after summing over the final states and averaging over the initial distribution, into an integral over time of the collisional TCF [Micha 1981, Micha and Vilallonga 1985]

$$\begin{aligned} R &= \int_{-\infty}^{+\infty} C_{TT}(t)\,dt \\ C_{TT}(t) &= \sum_n w_n \langle n|T^\dagger(0)T(t)|n\rangle \qquad (2.35) \\ \hat{T}(t) &= \exp\left(-iH_0 t/\hbar\right)T(0)\exp\left(iH_0 t/\hbar\right) \end{aligned}$$

where $\hat{H}_0$ is the Hamiltonian excluding the coupling between initial and final states, and w_n are statistical weights. The Dirac delta function in (2.34) assures the energy conservation in the system.

The existing theory must now be generalized to include the dissipative terms of the non Hermitian primary effective Hamiltonian (2.13) Due to their presence the total energy of the primary DFs is no longer conserved so the Fermi golden rule (2.34) is no longer valid The Appendix A presents details of the derivation of the state to state reaction rate for a system with dissipation [Beklíé and Micha to be publ] which becomes

$$R_{m\to n} = \frac{1}{\hbar}\left|\langle\tilde{\phi}_n^0|H_{pL}|\phi_m^0\rangle\right|^2 \frac{(W_m - W_n)}{(E_m - E_n)^2 + (W_m - W_n)^2/4} \qquad (2.36)$$

where $|\phi_m^0\rangle$ are right eigenstates of the non Hermitian Hamiltonian $H_0 = F_p + H_L$ and $\langle\tilde{\phi}_n^0|$ are their left counterparts Comparison of (2.34) and (2.36) reveals that the delta function in energy is substituted by a Lorentzian in energy whose width depends upon the dissipation strength parameters W_{es} and W_{ei} that are defined as expectation values of the dissipative Hamiltonian W^{φ} for the given eigenstates of $\hat{H}_0$. As will be shown in the next section, this generalization permits the expression of the photodesorption lineshape as a function of the dipole-dipole TCF.

The dipole-dipole TCF is a special case of the collisional TCF [Micha 1981, Micha and Vilallonga 1985], here $\hat{H}_0 = F_p + H_L$ and the transition operator $\hat{T}$ in the first order approximation of its Lippmann-Schwinger form [Schiff 1968] is $\hat{T} = \hat{H}_{pL} = -\hat{\vec{\mathcal{E}}} \cdot \vec{D}$. The dipole-dipole TCF is then

$$C_{DD}(t) = \langle \Upsilon_D(0) | \Upsilon_D(t) \rangle \tag{2.37}$$

with

$$\begin{aligned} |\Upsilon_D(t)\rangle &= \left[-\hat{\vec{\mathcal{E}}}(t) \cdot \vec{D}(t) \right] |\Psi(0)\rangle \\ \hat{\vec{\mathcal{E}}}(t) &= \exp\left(-iH_L t/\hbar\right) \hat{\vec{\mathcal{E}}}(0) \exp\left(iH_L t/\hbar\right) \\ \vec{D}(t) &= \exp\left(-iF_p t/\hbar\right) \vec{D}(0) \exp\left(iF_p t/\hbar\right) \end{aligned} \tag{2.38}$$

The quantized electric field $\hat{\vec{\mathcal{E}}}(t)$ is that of the incident light and it oscillates with time in the Heisenberg picture. It is assumed to be constant over space, which is quite realistic for visible and near UV wavelengths (order of magnitude of 100 nm) compared to the size of the region of the adsorption of the diatomic (order of magnitude of 0.1 nm). Also, as long the time dependence of the radiation field is purely oscillatory, i.e. $\hat{\vec{\mathcal{E}}}(t) = \hat{\varepsilon}_0 \exp\left(-i\omega_L t\right)$, which is the case for plain electromagnetic waves, it cancels out in the TCF expression (2.37) and the time dependence of the dipole amplitude (2.38) is governed by an effective frequency operator defined in terms of the primary effective Hamiltonian [Srivastava and

Micha [1991] i.e

$$|\Upsilon_D(t)\rangle = \exp\left[-i\left(\hat{P}_p - E\right)t/\hbar\right]|\Upsilon_D(0)\rangle \tag{2.39}$$

where E is the total initial energy of the primary region of the system.

The SCF formulation has been introduced for the transition dipole amplitude — it has been assumed that the transition dipole operator depends only on the primary degrees of freedom

$$D = \hat{D}(R, r) \tag{2.40}$$

so its time dependence is governed only by the primary DF Hamiltonian

The dipole amplitude is factored out [Srivastava and Micha 1 1991]

$$|\Upsilon(t)\rangle = |\xi(t)\rangle \ \ |\eta(t)\rangle \tag{2.41}$$

where the primary dipole amplitude is given by

$$|\xi(t)\rangle = \exp\left(-\frac{i}{\hbar}\hat{F}_p t\right)\left[\hat{D}|\psi^p(0)\rangle\right] \tag{2.42}$$

and $|\eta(t)\rangle = |\psi^s(t)\rangle$ is the secondary wavefunction The dipole-dipole TCF in the SCF formulation than becomes

$$\begin{gathered}
C_{DD}(t) = C^p_{DD}(t)C^s_{DD}(t) \\
C^p_{DD}(t) = \frac{\langle\xi(0)|\xi(t)\rangle}{|\langle\xi(0)|\xi(0)\rangle\langle\xi(t)|\xi(t)\rangle|^{1/2}} \\
C^s_{DD}(t) = \frac{\langle\eta(0)|\eta(t)\rangle}{|\langle\eta(0)|\eta(0)\rangle\langle\eta(t)|\eta(t)\rangle|^{1/2}}
\end{gathered} \tag{2.43}$$

Another quantity of interest is the autocorrelation function defined as

$$C(t) = \langle\Psi(0)|\Psi(t)\rangle \tag{2.44}$$

Again, the SCF type factorization can be introduced and each factor is obtained from the corresponding region wavefunction itself, hence,

$$
\begin{aligned}
C(t) &= C^p(t)C^s(t) \\
C^p(t) &= \frac{\langle\psi^p(0)|\psi^p(t)\rangle}{|\langle\psi^p(0)|\psi^p(0)\rangle\langle\psi^p(t)|\psi^p(t)\rangle|^{1/2}} \\
C^s(t) &= \frac{\langle\psi^s(0)|\psi^s(t)\rangle}{|\langle\psi^s(0)|\psi^s(0)\rangle\langle\psi^s(t)|\psi^s(t)\rangle|^{1/2}}
\end{aligned}
\qquad (2.45)
$$

where the separate normalization is necessary for each factor because they evolve over time with non Hermitian complex Hamiltonians

Photodesorption Lifetime and Lineshape in terms of the TCFs

At the beginning of the previous section it was stated that certain physical properties of the system of interest can be expressed in terms of time correlation functions In this section it will be shown how the photodesorption lifetime of the Ni(001)(ads)CO system can be deduced from the autocorrelation function while a generalized photodesorption lineshape including the energy dissipation in the substrate, can be written as a temporal Fourier transform of the dipole-dipole TCF

The absolute value square of the autocorrelation function (2.39) is also known as the survival probability amplitude (SPA) Its decay rate is a measure of the lifetime of the specified initial state of the system In this case, the decay rate is computed for the primary SPA assuming its exponential decay $C^p(t) = C^p(0)\exp(-t/\tau)$, it is defined by the following expression

$$\tau = 2\int_0^\infty \frac{d\,|C^p(t)|^2}{dt}\,t\,dt \qquad (2.46)$$

For physical systems coupled to an environment, the assumption of exponential decay is applicable only in the absence of such coupling i e at a late time limit

Therefore after taking a natural logarithm of the exponential decay law

$$\ln\left[C^{p}(t)\right] = \ln\left[C^{p}(0)\right] - t/\tau \tag{2.47}$$

it becomes obvious that the lifetime of the desorbing state can be estimated as the inverse negative slope of $\ln\left[C^{p}(t)\right]$ in the asymptotic time limit.

The photodesorption lineshape for a nondissipative desorbing state was defined as a time Fourier transform of the dipole-dipole TCF [Srivastava and Micha I 1991]

$$L(\omega) = \frac{1}{4\pi^2}\left|\int_0^\infty C_{DD}(t)\exp(\imath\omega t)dt\right|^2 \tag{2.48}$$

where $C_{DD}(t)$ was defined by the eqn. (2.37). An analogous expression must now be derived to include the dissipation in the substrate.

The derivation starts from the state-to-state rate constant (2.36) with the Lorentzian in energy expressed as a time integral

$$\frac{(W_m - W_n)}{(E_m - E_n)^2 + (W_m - W_n)^2/4} = \frac{2}{\hbar}Re\int_0^\infty e^{-i[(E_m-E_n)-\imath(W_m-W_n)/2]t/\hbar}dt \tag{2.49}$$

so that

$$R_{m\to n} = \frac{2}{\hbar^2}Re\int_0^\infty \langle\phi_m^0|\bar{H}_{pL}|\phi_n^0\rangle \times \times e^{\imath(E_n-\imath W_n/2)t/\hbar}\langle\bar{\phi}_n^0|H_{pL}|\phi_m^0\rangle e^{-\imath(E_m-\imath W_m/2)t/\hbar}dt \tag{2.50}$$

Recalling that $|\phi_m^0\rangle$ are eigenstates of the operator $F_0 = (H_p - \imath W_p/2) + H_L$, they can be written as direct products of the eigenstates of the adsorbate-substrate complex and the eigenstates of the radiation field Hamiltonian. This means that

$$|\phi_m^0\rangle e^{-\imath(E_m-\imath W_m/2)t/\hbar} = e^{-\imath\left(\hat{H}_p-\imath\hat{W}_p/2\right)t/\hbar}|\psi^p_{m_p}\rangle \otimes |m_R\rangle e^{-\imath\omega t/\hbar} \tag{2.51}$$

with an analogous expression for the left eigenvector $\langle\tilde{\phi}^0_n|$, here $|\psi^0_{m_p}\rangle$ are the eigenstates of the primary dissipative Hamiltonian without the radiation field with quantum numbers m_p, and $|m_{\mathcal{E}}\rangle$ are the photon number eigenstates of the radiation field Hamiltonian. From eqns. (2.13) and (2.14) it follows that the matrix elements of the system-radiation coupling $\hat{H}_{pL}$ in the basis of photon number eigenstates are given by

$$\langle n_{\mathcal{E}}|\hat{H}_{pL}|m_{\mathcal{E}}\rangle = i\sqrt{\frac{\omega_{\mathcal{E}}}{2\varepsilon_0}}\hat{D}_y(\vec{X})(\delta_{n_{\mathcal{E}},m_{\mathcal{E}}-1} - \delta_{n_{\mathcal{E}},m_{\mathcal{E}}+1}) = D_p^{m_{\mathcal{E}},n_{\mathcal{E}}} \tag{2.52}$$

Introducing (2.52) and (2.53) into (2.51), and defining the photodesorption lineshape for the one-photon absorption processes as a total rate for the *molecular* states

$$L(\omega_{\mathcal{E}}) = \sum_{m_p} w_{m_p} \sum_{n_p} R_{\{m_p,\, m_{\mathcal{E}}=1 \rightarrow n_p,\, n_{\mathcal{E}}=0\}} \tag{2.53}$$

the lineshape becomes

$$\begin{aligned} L(\omega_{\mathcal{E}}) = \frac{2}{\hbar^2} Re \sum_{m_p} w_{m_p} \int_0^{\infty} \langle\psi^p_{m_p}|D_p^{1,0}(0)|\times \\ \times\left(\sum_{n_p}|\tilde{\psi}^p_{n_p}\rangle\langle\tilde{\psi}^p_{n_p}|\right) D_p^{1,0}(t)|\psi^p_{m}\rangle e^{-i\omega_{\mathcal{E}}t}dt \end{aligned} \tag{2.54}$$

where

$$D_p^{1,0}(t) = e^{i(\hat{H}_p - i\hat{W}_p/2)t/\hbar} D_p^{1,0} e^{-i(\hat{H}_p - i\hat{W}_p/2)t/\hbar} \tag{2.55}$$

and the photon number indices have been omitted. In analogy with the analysis of Appendix A, the left eigenstate $|\tilde{\psi}^p_{n_p}\rangle$ can be written in terms of its right counterpart and again, if the dissipation is relatively weak, it can be approximated by $|\psi^p_{n_p}\rangle$ in the eqn. (2.55). The summation over n_p then yields an identity and after averaging over the initial distribution of the adsorbate-substrate complex eigenstates the photodesorption lineshape becomes

$$L(\omega) = \int_{0}^{\infty} C_{DD}(t) \exp(-i\omega t) dt \qquad (2.56)$$

having omitted the photon indices n_g and m_g with

$$C_{DD}(t) = \frac{2}{\hbar^2} \langle\langle D_\rho(0) \bar{D}_\rho(t) \rangle\rangle \qquad (2.57)$$

CHAPTER 3
DYNAMICS OF THE SECONDARY DEGREES OF FREEDOM

Classification of Secondary DF Excitations

As the secondary region in this study is a metal surface, there are two common ways of excitations that lead to energy dissipation through density and charge fluctuations in it: lattice vibrations — phonons, and electronic excitations. Consequently, the secondary degree of freedom (DF) Hamiltonian is expressed as a sum of two terms

$$H_s = H_s^v + H_s^e \tag{3.1}$$

and the coupling to the primary DFs is a sum of two terms as well, not accounting for the electron-phonon interactions for simplicity, so that

$$\hat{H}_{ps} = H_{ps}^v + H_{ps}^e \tag{3.2}$$

To specify the Hamiltonian in more detail, the coordinates of substrate and adsorbate atoms must be chosen. Two different choices are obvious: the first one would be appropriate for the bound adsorbate and would consist of the vibrational normal coordinates for the whole system; the second choice introduces the normal coordinates $Q_{\vec{k}}$ of the metal without the adsorbate, and the Jacobi (center of mass) coordinates $\vec{X}$ for the adsorbate relative to the metal surface. In the present study of desorption, the second choice is more convenient.

The secondary DF Hamiltonian for any boson type excitation, phonons included is now rewritten as

$$H_s^s = \sum_\nu \omega_\nu \left(\hat{N}_\nu + \frac{1}{2}\hat{I} \right) \quad (3.3)$$

where ω_ν are characteristic frequencies of the secondary region states labeled by quantum numbers ν, and $\hat{N}_\nu$ are the occupation number operators of those states which can be written in terms of creation and annihilation operators as

$$\hat{N}_\nu = \hat{b}_\nu^\dagger \hat{b}_\nu \quad (3.4)$$

The excitation operators $\hat{b}_\nu^\dagger$ and $\hat{b}_\nu$ are boson type operators that satisfy the commutation rule [Kittel 1963]

$$\left[\hat{b}_\nu^\dagger, \hat{b}_\mu\right] = \delta_{\nu,\mu} \hat{I} \quad (3.5)$$

where $\hat{I}$ is the identity operator

The coupling Hamiltonian to the primary DFs is first rewritten in the basis of primary diabatic electronic states (to be defined in Chapter 4)

$$H_{ps}^s = \sum_{I=1}^{N} \sum_{J=1}^{N} |\psi_I^d(\vec{X})\rangle H_{I,J}^{ps}(\vec{X}) \langle \psi_J^d(\vec{X})| \quad (3.6)$$

where $H_{I,J}^{ps}(\vec{X})$ are matrix elements in the basis of primary diabatic electronic states that depend on the primary degrees of freedom they form the N by N (in this particular case N=2) matrix operators Each of these matrix elements can now be written in a general form as a sum over all the excitations involving the secondary DFs

$$\hat{H}_{I,J}^{ps} = \sum_\nu \left[\left(\hat{b}_\nu^\dagger + \hat{b}_\nu \right) H_{I,J}^\nu(\vec{X}) + \sum_\lambda \frac{1}{2} \left(\hat{b}_\nu^\dagger + \hat{b}_\nu \right) \left(\hat{b}_\lambda^\dagger + \hat{b}_\lambda \right) H_{I,J}^{\nu\lambda}(\vec{X}) \right] \quad (3.7)$$

where $\hat{b}_\nu$ and $\hat{b}_\nu{}^\dagger$ are the corresponding excitation operators and $H^{\nu}{}_{IJ}$ and $H^{\nu\lambda}{}_{IJ}$ are the linear and bilinear coupling parameters for each pair of the electronic states' transitions.

The next task is to derive the equations of motion for the secondary DFs excitation operators, they must be Heisenberg equations of motion with the secondary DF effective Hamiltonian, defined in Chapter 2

$$i\frac{d}{dt}b_\mu^\dagger = \left[\hat{F}_s^{\nu}(t), b_\mu^\dagger\right] \tag{3.8}$$

and a similar equation for $\hat{b}_\mu$. The effective Hamiltonian for the secondary DFs is given by

$$F_s^{\nu}(t) = \hat{H}_s^{\nu} + \langle\psi^p(t)|H^{\nu}_{ps}|\psi^p(t)\rangle / \langle\psi^p(t)|\psi^p(t)\rangle \tag{3.9}$$

so introducing $\hat{H}_s{}^\nu$ and $H_{ps}{}^\nu$ it can be written as

$$\begin{aligned} F_\nu^{\nu}(t) = \sum_\nu \omega_\nu\left(\hat{b}_\nu^\dagger b_\nu + \frac{1}{2}I\right) + \\ + \sum_\nu\left[h_\nu(t)\left(b_\nu^\dagger + b_\nu\right) + \sum_\lambda \frac{1}{2}h_{\nu,\lambda}(t)\left(b_\nu^\dagger + b_\nu\right)\left(b_\lambda^\dagger + \hat{b}_\lambda\right)\right] \end{aligned} \tag{3.10}$$

The time dependent coupling parameters are given by

$$h_\nu(t) = \sum_I\sum_J \langle\psi_I^p(t)|H^{\nu}_{I,J}|\psi_J^p(t)\rangle / \sum_I \langle\psi_I^p(t)|\psi_I^p(t)\rangle \tag{3.11}$$

and

$$h_{\nu\lambda}(t) = \sum_I\sum_J \langle\psi_I^p(t)|H^{\nu\lambda}_{I,J}|\psi_J^p(t)\rangle / \sum_I \langle\psi_I^p(t)|\psi_I^p(t)\rangle \tag{3.12}$$

Evaluating the commutator in the Heisenberg equation for $\hat{b}_\mu{}^\dagger$ yields

$$i\frac{d}{dt}b_\mu^\dagger(t) + \omega_\mu\hat{b}_\mu^\dagger(t) + \sum_\nu \frac{1}{2}[h_{\mu\nu}(t) + h_{\nu\mu}(t)]\left[b_\nu^\dagger(t) + b_\nu(t)\right] + h_\mu(t)I = 0 \tag{3.13}$$

and the Hermitian adjoint equation for $\hat{b}_\mu$. Obviously, $\hat{b}_\mu^\dagger$ and $\hat{b}_\mu$ are coupled in these equations and decoupling them is not simple with time dependent coupling parameters (3.11) and (3.12).

It is useful at this point to introduce new operators for mass weighted secondary coordinates and conjugate momenta defined as linear combinations of the creation and annihilation operators

$$\hat{Q}_\nu = \frac{1}{\sqrt{2\omega_\nu}}\left(\hat{b}_\nu^\dagger + \hat{b}_\nu\right) \tag{3.14}$$

and

$$P_\nu = i\sqrt{\frac{\omega_\nu}{2}}\left(\hat{b}_\nu^\dagger - \hat{b}_\nu\right) \tag{3.15}$$

These coordinates and momenta represent the substrate normal modes without the presence of the adsorbate, and they satisfy the commutation relation

$$\left[\hat{P}_\mu, \hat{Q}_\nu\right] = i\delta_{\mu,\nu} I \tag{3.16}$$

The secondary DF effective Hamiltonian can be rewritten in terms of $\hat{Q}_\nu$ and $\hat{P}_\nu$, so it becomes

$$F_s(t) = \sum_\nu \left[\frac{1}{2}P_\nu^2 + \frac{\omega_\nu^2}{2}Q_\nu^2 + h_\nu(t)\hat{Q}_\nu + \sum_\lambda \frac{1}{2}h_{\nu,\lambda}(t)Q_\nu\hat{Q}_\lambda\right] \tag{3.17}$$

The solution of the time-dependent Schroedinger equation for this Hamiltonian is a superposition of vibrational states describing a collection of normal modes ν with occupation numbers n_ν so that

$$|\psi_\beta^s(t)\rangle = \sum c_\beta(\{n_\nu\}, t)|\{n_\nu\}\rangle \tag{3.18}$$

Now, instead of solving the Heisenberg equations for the creation and annihilation operators, it is more practical to solve the analogous equations for the coordinates and conjugate momenta, using the effective Hamiltonian (3 17) After evaluating the commutators the coupled differential equations for $\hat{Q}_\mu$ and $\hat{P}_\mu$ are

$$\frac{d}{dt}\hat{Q}_\mu(t) = P_\mu(t) \tag{3.19}$$

and

$$\frac{d}{dt}P_\mu(t) + \omega_\mu^2 \hat{Q}_\mu(t) + \sum_\lambda \frac{1}{2}\left[h_{\mu,\lambda}(t) + h_{\lambda,\mu}(t)\right] Q_\lambda(t) + h_\mu(t)\hat{I} = 0 \tag{3.20}$$

These equations can be decoupled simply by taking a time derivative of the former and inserting the result into the left hand side of the latter the final result is a set of parametrically coupled driven harmonic oscillator equations in $\hat{Q}_\mu$

$$\frac{d^2}{dt^2}\hat{Q}_\mu(t) + \omega_\mu^2 \hat{Q}_\mu(t) + \sum_\lambda \frac{1}{2}\left[h_{\mu,\lambda}(t) + h_{\lambda,\mu}(t)\right] Q_\lambda(t) + h_\mu(t)\hat{I} = 0 \tag{3.21}$$

The square bracket in the third term contains the square of the time dependent part of the frequency and the coupling between the modes, while the last term is the driving force However, coupling of different modes through the time dependent frequency presents a difficulty in solving for the time dependence of the phonon coordinate operators This can be circumvented by making another coordinate transformation in order to diagonalize the above system of equations which is equivalent to the normal mode analysis In that case $h_{\mu,\lambda}(t) = h_{\lambda,\mu}(t) = h_{\mu,\mu}(t)\delta_{\mu,\lambda}$ so the coupling of modes disappears The decoupled equations of motion then read

$$\frac{d^2}{dt^2}Q_\mu(t) + \left[\omega_\mu^2 + h_{\mu,\mu}(t)\right] Q_\mu(t) + h_\mu(t) I = 0 \tag{3.22}$$

for each normal mode μ The solution to these equations can be written in terms of pairs of linearly independent solutions of the corresponding homogeneous equations

$$\left[\frac{d^2}{dt^2} + \Omega_\mu^2(t)\right]\left\{\begin{matrix} f_\mu(t) \\ g_\mu(t) \end{matrix}\right\} = 0 \qquad (3\ 23)$$

where by definition $\Omega_\mu(t) = \sqrt{\omega_\mu^2 + h_{\mu,\mu}(t)}$, and the initial conditions are chosen as

$$\begin{aligned} f_\mu(0) &= 0\ , \qquad (df_\mu/dt)_0 = \Omega_\mu(0) \\ g_\mu(0) &= 1\ , \qquad (dg_\mu/dt)_0 = 0 \end{aligned} \qquad (3.24)$$

These initial conditions reflect the fact that the adsorbate is initially bound to the substrate so that the time derivative$(df_\mu/dt)_0$ is equal to the initial value of the modified frequency of the μth substrate normal mode

The solution for the μth normal mode [Yamashita and Miller 1985 Srivastava and Micha I 1991] is

$$\hat{Q}_\mu(t) = Q_\mu(0)g_\mu(t) + \frac{P_\mu(0)}{\omega_\mu}f_\mu(t) - \int_0^t \frac{1}{\omega_\mu}\hat{h}_\mu(t')f_\mu[(t-t')]dt' \qquad (3\ 25)$$

If the bilinear coupling terms are neglected altogether, the time dependence in the frequencies disappears and the functions f_μ and g_μ become *sin($\omega_\mu t$)* and *cos($\omega_\mu t$)* respectively

As stated in the beginning of this section, the creation and annihilation operators $\hat{b}_\mu{}^\dagger$ and $\hat{b}_\mu$ can fully describe any boson type excitations in the substrate, such as phonons It is worth noting that this approach may be generalized also to the electronic excitations if they can be understood as electron hole pair excitations [March et al 1967] however the physical interpretation of terms in the effective Hamiltonian is then very different because the lowest term i.e excluding couplings to the primary DFs and to other secondary DFs' excitations is then linear in the electron hole operators rather than bilinear in the boson type operators of elementary excitations. Those operators must be defined as linear combinations of the pair creation and annihilation operators, with the coefficients depending upon the form of the Hamiltonian.

Quantum Dynamics of the Secondary Degrees of Freedom: Electronic Excitations

In this section, electronic excitations in the substrate will be treated separately as fermion type excitations. The model will include only the one electron processes, allowing for the description of the conduction and the upper empty band of the substrate, and the transitions within and between them.

In order to describe the substrate electronic states, one must first define the fermionic creation and annihilation operators. For a single metal band, these operators satisfy the relations

$$\hat{a}^{\dagger}_{\bar{k}}|\text{vac}\rangle = |\bar{k}\rangle \tag{3.26}$$

and

$$\hat{a}_{\bar{k}}|\bar{k}\rangle = |\text{vac}\rangle \tag{3.27}$$

where $|\bar{k}\rangle$ is a single electron state with quasi momentum $\bar{k}$ and energy $\varepsilon_{\bar{k}}$, while $|\text{vac}\rangle$ is the vacuum state with no electrons present.

The above operators satisfy the anticommutation rules

$$\left[\hat{a}^{\dagger}_{\bar{k}}, \hat{a}_{\bar{k}'}\right]_{+} = \delta\left(\bar{k} - \bar{k}'\right)I \tag{3.28}$$

and

$$\left[\hat{a}^{\dagger}_{\bar{k}}, \hat{a}^{\dagger}_{\bar{k}'}\right]_{+} = \left[\hat{a}_{\bar{k}}, \hat{a}_{\bar{k}'}\right]_{+} = 0 \tag{3.29}$$

These anticommutation rules are equivalent to the Pauli exclusion principle for fermions [Kittel 1963].

The elementary excitations in this system are the electron-hole pairs created by the boson like operators $B_{\vec{k}\vec{k}'} = a^{\dagger}_{\vec{k}} a_{\vec{k}'}$. These satisfy the rules of a unitary Lie algebra [March et al. 1967, Paldus and Čížek 1975], which can be used to derive their equations of motion. A simpler approach is taken here, similar to the time-dependent Hartree-Fock description of the dielectric properties of a many electron system driven by an electromagnetic field [Ehrenreich and Cohen 1959] but related instead to the driving effect of the desorbing species [Ziman 1960].

The simplest physical model for the secondary DFs includes only the single particle terms in the effective Hamiltonian. The secondary Hamiltonian is given by

$$H^{s}_{s} = \sum_{\vec{k}} \epsilon_{\vec{k}} a^{\dagger}_{\vec{k}} a_{\vec{k}} \tag{3.30}$$

while the primary secondary coupling Hamiltonian, expanded in the basis of the primary diabatic electronic states from Chapter 4, reads

$$H^{s}_{ps} = \sum_{I,J} |\psi^{d}_{I}(\vec{X})\rangle \sum_{\vec{k}} \sum_{\vec{k}'} H^{I,J}_{\vec{k}\vec{k}'}(\vec{X}) a^{\dagger}_{\vec{k}} a_{\vec{k}'} \langle \psi^{d}_{J}(\vec{X})| \tag{3.31}$$

Replacing this expression into the equation for the effective secondary Hamiltonian,

$$F^{s}_{s}(t) = \sum_{\vec{k}} \epsilon_{\vec{k}} a^{\dagger}_{\vec{k}} a_{\vec{k}} + \sum_{\vec{k}} \sum_{\vec{k}'} h_{\vec{k}\vec{k}'}(t) a^{\dagger}_{\vec{k}} a_{\vec{k}'} \tag{3.32}$$

with

$$h_{\vec{k}\vec{k}'}(t) = \sum_{I,J} \langle \psi^{\eta}_{I}(t) | H^{I,J}_{\vec{k}\vec{k}'} | \psi^{\eta}_{J}(t) \rangle \Big/ \sum_{I} \langle \psi^{\eta}_{I}(t) | \psi^{\eta}_{I}(t) \rangle \tag{3.33}$$

where the second term includes interaction energies of quasiparticle states due to the presence of the adsorbate [Brako and Newns 1989]. Ranges of the summations will depend on specific choices, e.g. conduction or empty band of the substrate metal.

The secondary DFs are described by a time dependent many-electron density operator defined in terms of the secondary many-electron wavefunction

$$\Gamma^{\beta}_{s}(t) = |\psi^{s}_{\beta}(t)\rangle\langle\psi^{s}_{\beta}(t)|$$
$$|\psi^{s}_{\beta}(t)\rangle = \sum_{\vec{k}_1,\ldots,\vec{k}_N} c_{\beta}\left(\vec{k}_1,\ldots,\vec{k}_N,t\right)|\vec{k}_1,\ldots,\vec{k}_N\rangle \qquad (3.34)$$

where the state $|\psi^{s}_{\beta}(t)\rangle$ is an N-electron wavefunction that solves the time dependent Schroedinger equation with the effective electronic Hamiltonian $\hat{F}^{e}_{s}$, and is given by a time-dependent superposition of Slater determinants made up of N quasiparticle states. In the TDHF approximation, that state reduces to a single Slater determinant $\psi^{s}_{\beta} = \psi^{s}_{HF}$ made up of N time dependent spin-orbitals

If only one-electron processes are of interest, the many-electron density can be adequately given by the reduced or one-electron density operator, which can be defined as [March et al 1967]

$$\varrho_{s}(t) = Tr_{2\ldots N}\left[\Gamma^{\beta}_{s}(t)\right] = \sum_{\vec{k}}\sum_{\vec{k}'} \varrho_{\vec{k}\vec{k}'}(t) a^{\dagger}_{\vec{k}} a_{\vec{k}'} \qquad (3.35)$$

This density operator must satisfy the Liouville Von Neuman equation with the secondary DF effective Hamiltonian

$$i\frac{d}{dt}\varrho_{s}(t) = \left[\hat{F}^{e}_{s}(t), \varrho_{s}(t)\right] \qquad (3.36)$$

Similarly to the case of phonons the one-electron density matrix elements $\varrho_{\vec{k}\vec{k}'}(t)$ are evaluated in the basis of quasiparticle electronic states $|\vec{k}\rangle$ of the isolated solid without the adsorbate

Introducing the density operator (3.35) and the effective Hamiltonian (3.32) into the Liouville eqn (3.36) evaluating the right hand side with the use of the anticommutation rules (3.28) and (3.29), and collecting terms yields a set of coupled time dependent differential equations for the one-electron density matrix elements

$$i\frac{d}{dt}\varrho_{\vec{k}\vec{k}'}(t) = (\varepsilon_{\vec{k}} - \varepsilon_{\vec{k}'})\varrho_{\vec{k}\vec{k}'}(t) + \sum_{\vec{k}''}\left[h_{\vec{k}\vec{k}''}(t)\varrho_{\vec{k}''\vec{k}'}(t) - h_{\vec{k}''\vec{k}'}(t)\varrho_{\vec{k}\vec{k}''}(t)\right] \tag{3.37}$$

for each pair of values $(\vec{k},\vec{k}')$

To the lowest order neglecting the coupling altogether, the above set of equations has a simple oscillatory solution

$$\varrho^{(0)}_{\vec{k}\vec{k}'}(t) = \exp\left[-i(\varepsilon_{\vec{k}} - \varepsilon_{\vec{k}'})t\right]\varrho^{(0)}_{\vec{k}\vec{k}'}(0) \tag{3.38}$$

When the coupling is included, the equations of motion for the one-electron density matrix elements can be solved using the metal dielectric function if the coupling is weak [Kittel 1963] or e.g. by temporal linearization [Micha and Runge 1992] if the coupling is strong. The operator solution is given in terms of the time-evolution operator for this potential as

$$\rho_s(t) = \hat{U}_s(t,0)\hat{\rho}_s(0)U_s(t,0)^{\dagger} \tag{3.39}$$

As in the case of phonons, initial conditions must be specified taking into account that the adsorbate is bound to the substrate at the initial time.

Form of the Primary-Secondary DF Coupling Hamiltonian

In this section the primary-secondary DF coupling Hamiltonian is derived in terms of the solutions to the secondary DF dynamics for both phonons and electrons. Then using the definitions from Chapter 2, the form of the primary

DF imaginary potentials is obtained, thus the assumptions made in solving for the primary DF quantum dynamics are justified.

The coupling Hamiltonian for the case of phonons, including the assumption that the phonon coordinates are uncoupled (i.e. that they are in fact normal mode coordinates), is given by

$$H^{\nu}_{ps} = \sum_{I,J} |\psi^{s}_{I}(\vec{X})\rangle \sum_{\nu} \left[H^{\nu}_{I,J}(\vec{X}) Q_{\nu} + H^{\nu\nu}_{I,J}(\vec{X}) Q^{2}_{\nu} \right] \langle\psi^{s}_{J}(\vec{X})| \tag{3.40}$$

To evaluate its expectation value with respect to the secondary DFs, one must find the expectation values

$$\langle Q_{\nu}(t)\rangle_{\beta} = \langle\psi^{s}_{\beta}(t)|Q_{\nu}|\psi^{s}_{\beta}(t)\rangle / \langle\psi^{s}_{\beta}(t)|\psi^{s}_{\beta}(t)\rangle = q^{\beta}_{\nu}(t) \tag{3.41}$$

and

$$\langle Q^{2}_{\nu}(t)\rangle_{\beta} = \langle\psi^{s}_{\beta}(t)|Q^{2}_{\nu}|\psi^{s}_{\beta}(t)\rangle / \langle\psi^{s}_{\beta}(t)|\psi^{s}_{\beta}(t)\rangle = q^{\beta}_{2\nu}(t) \tag{3.42}$$

Using the solution (3.25), these expectation values can be written in terms of their own initial values, omitting for now the subscript β, as

$$q_{\nu}(t) = q_{\nu}(0) g_{\nu}(t) + \frac{p_{\nu}(0)}{\omega_{\nu}} f_{\nu}(t) - \int_{0}^{t} \frac{h_{\nu}(t')}{\omega_{\nu}} f_{\nu}(t-t') dt' \tag{3.43}$$

and

$$q_{2\nu}(t) = \langle Q_{\nu}(0)^{2}\rangle g_{\nu}(t)^{2} + \frac{\langle P_{\nu}(0)^{2}\rangle}{\omega^{2}_{\nu}} f_{\nu}(t)^{2} - \left[\int_{0}^{t} \frac{h_{\nu}(t')}{\omega_{\nu}} f_{\nu}(t-t') dt' \right]^{2} +$$
$$+2\left\{ \frac{\langle Q_{\nu}(0) P_{\nu}(0)\rangle}{\omega_{\nu}} f_{\nu}(t) g_{\nu}(t) - \left[q_{\nu}(0) g_{\nu}(t) + \frac{p_{\nu}(0)}{\omega_{\nu}} f_{\nu}(t) \right] \int_{0}^{t} \frac{h_{\nu}(t')}{\omega_{\nu}} f_{\nu}(t-t') dt' \right\} \tag{3.44}$$

The initial values in these expressions refer to the substrate perturbed by the adsorbate and must be obtained from the statistical averages for that situation.

Finally the expectation value of the coupling Hamiltonian (3.7) can be written in terms of (3.41) and (3.42) so it becomes

$$h_p^v = \sum_{IJ} |\psi_I^a(\vec{X})\rangle h_{IJ}^v(\vec{X},t)\langle\psi_J^a(\vec{X})|$$

$$h_{IJ}^v(\vec{X},t) = \sum_\nu \left[H_\nu^{IJ}(\vec{X}) q_\nu(t) + \frac{1}{2} H_{\nu\nu}^{IJ}(\vec{X}) q_{2\nu}(t) \right] \tag{3.45}$$

This expression shows that the coupling between the primary electronic states and the metal lattice vibrations will be oscillating rapidly due to the summation over normal mode contributions.

The matrix elements of couplings between different electronic states of the adsorbate come from the momentum couplings of the Born-Oppenheimer theory; after the transformation from the adiabatic to the diabatic representation, they are likely to be small except at crossings or avoided crossings and are likely to depend only weakly on lattice displacements, therefore a good assumption is that the coupling matrix is diagonal in the electronic labels and linear in the displacements, giving

$$h_p^{(\beta)} = \sum_I |\psi_I^a(\vec{X})\rangle h_{II}^{(\beta)}(\vec{X},t)\langle\psi_I^a(\vec{X})| \tag{3.46}$$

$$h_{II}^\beta(\vec{X},t) = \sum_\nu H_\nu^{II}(\vec{X}) q_\nu^\beta(t) \tag{3.47}$$

where the secondary state index β has been restored. The vibrational excitations of the substrate would therefore contribute to the random forces and dissipation in the electronically adiabatic motion of the adsorbate but would not contribute to electronic transitions. Expressions similar to the one above have been frequently used in the literature to model coupling to a vibrating lattice [Messina and Coalson

1991] The formulation in this study adds the effect of the SCF coupling to the primary DFs, as it appears in the third term of Eq (3 21), this term modifies the harmonic oscillation of the ν–th mode, and introduces a different anharmonicity for each vibrational state β of the lattice

The primary secondary DF coupling Hamiltonian for the secondary electronic states expanded in the basis of the primary diabatic electronic states, reads

$$\hat{H}^{e}_{ps} = \sum_{I,J} |\psi^{e}_{I}(\vec{X})\rangle \sum_{\vec{k}} \sum_{\vec{k}'} H^{I,J}_{\vec{k},\vec{k}'}(\vec{X}) \hat{a}^{\dagger}_{\vec{k}} \hat{a}_{\vec{k}'} \langle\psi^{e}_{J}(\vec{X})| \qquad (3\ 48)$$

Since the secondary DFs are now described by the one-electron density operator evaluating the expectation value of the Hamiltonian (3.31) with respect to the secondary DFs is equivalent to calculating its trace with respect to the one electron density, i e.

$$h^{e}_{p}(t) = \frac{Tr_{s}\left[\rho_{s}(t)\hat{H}^{e}_{ps}\right]}{Tr_{s}\left[\rho_{s}(t)\right]} \qquad (3\ 49)$$

and evaluating the trace one finds

$$\begin{aligned} h^{e}_{p} &= \sum_{I J} |\psi^{e}_{I}(\vec{X})\rangle h^{e}_{IJ}\left(\vec{X},t\right)\langle\psi^{e}_{J}(\vec{X})| \\ h^{e}_{IJ}\left(\vec{X}\ t\right) &= \sum_{\vec{k}} \sum_{\vec{k}'} \rho_{\vec{k},\vec{k}'}(t) H^{I,J}_{\vec{k}',\vec{k}}(\vec{X}) / \sum_{\vec{k}} \rho_{\vec{k},\vec{k}}(t) \end{aligned} \qquad (3\ 50)$$

As is evident from the solution (3 38) this trace is a sum of terms with oscillatory time dependence and the characteristic frequencies come from intraband electron hole excitations These frequencies are usually smaller than the differences of molecular electronic energies and would not contribute to electronic transitions during desorption but would appear as random forces and dissipation in the adsorbate adiabatic motion The sum over electron hole excitations in the coupling leads to a very rapidly varying trace so that the fluctuation and memory terms (2.27) and (2.28) of the primary effective Hamiltonian should show the time dependence typical of Brownian motions.

The treatment above can be extended to include interband transitions. In this case the quasiparticle states must be labelled by the band indices $b = C, U$ for the conduction and unoccupied bands respectively, in addition to the quasi momentum label. A new index $\lambda = (b, \vec{k})$ can be used to write the more general matrix elements of the coupling and the density matrix. The double sums in h^{c}_{IJ} can be rewritten as the sum of terms relating to the conduction intraband transitions, plus terms relating to interband $C \rightarrow U$ and $C \leftarrow U$ transitions. The SCF coupling in the primary states can be written, restoring the β index, as

$$\hat{h}^{(\beta)}_{p} = \sum_{I,J} |\psi^{\beta}_{I}(\vec{X})\rangle h^{(\beta)}_{IJ}\left(\vec{X}, t\right)\langle\psi^{\beta}_{J}(\vec{X})| \tag{3.51}$$

$$\begin{aligned} h^{(\beta)}_{IJ}\left(\vec{X}, t\right) &= \sum_{\lambda}\sum_{\lambda'} \gamma^{\beta}_{\lambda,\lambda'}(t) H^{IJ}_{\lambda',\lambda}(\vec{X}) \\ \gamma^{\beta}_{\lambda,\lambda'}(t) &= \rho^{\beta}_{\lambda,\lambda'}(t) / \sum_{\lambda} \rho^{\beta}_{\lambda,\lambda}(t) \end{aligned} \tag{3.52}$$

in terms of a normalized electron density matrix γ.

The potential matrix elements $H^{IJ}_{\lambda'\lambda}$ derive from both the diabatic coupling between electronic and nuclear motions, and from the Coulomb interaction among electrons. They are larger when the adsorbate electronic state is the same, $I = J$, because then there is a larger overlap of the total electronic states. For $I \neq J$ there is also an interaction, with a longer range than vibrational couplings because the present electronic couplings have a Coulombic origin.

So far the treatment of the secondary DFs has considered the boson-like excitation operators $\{B_j\} = \{\hat{Q}_j, P_j\}$ for the lattice vibrations and $\{B_j\} =$

$\{a_j^\dagger a_j\}$ for the electron hole excitations To complete the treatment of electronic excitations in the substrate one should also consider the coupling of e h excitations with lattice vibrations This can be done introducing collective excitation operators $\{B_j\} = \{a_\lambda^\dagger a_\lambda Q_\mu \ , \ a_\lambda^\dagger a_\lambda P_\mu\}$, which combine electron hole and phonon operators, and proceeding as before. However, this shall not be done for sake of simplicity instead, the effective primary Hamiltonian will be constructed for the previous two cases

Form of the Primary DF Energy Dissipation Operator

From the definition in Chapter 2 for the energy fluctuation and memory terms, introducing now the state index β for the secondary states

$$R_p^{(\beta)}(t) = \frac{\langle \psi_\beta^s(t) | \tilde{H}_{ps} | \psi_\beta^s(t) \rangle}{\langle \psi_\beta^s(t) | \psi_\beta^s(t) \rangle} \exp(-i\tilde{H}_p t/\hbar) \tag{3.53}$$

and

$$M_p^{(\beta)}(t,t') = \frac{\langle \psi_\beta^s(t) | H_{ps} | \psi_\beta^s(t) \rangle}{\langle \psi_\beta^s(t) | \psi_\beta^s(t) \rangle} \exp[-iH_p(t-t')/\hbar] \frac{\langle \psi_\beta^s(t') | H_{ps} | \psi_\beta^s(t') \rangle}{\langle \psi_\beta^s(t') | \psi_\beta^s(t') \rangle} \tag{3.54}$$

These operators may be obtained for substrate phonons or for e h excitations and can be averaged over the statistical distributions of secondary states β In both cases they are given in terms of the expectation values of the collective motion operators by

$$\begin{aligned} h_p^{(\beta)} &= \sum_j H_j(\hat{X}) b_j^\beta(t) \\ b_j^\beta(t) &= \langle B_j(t) \rangle_\beta \end{aligned} \tag{3.55}$$

The statistical averages of fluctuation and dissipation terms are then

$$\begin{aligned} R_p(t) &= \sum_j \langle\langle b_j(t)\rangle\rangle H_j(\bar{X}) \exp(-i\hat{H}_p t/\hbar) \\ \langle\langle b_j(t)\rangle\rangle &= \sum_\beta w_\beta b_j^\beta(t) \end{aligned} \tag{3.56}$$

and

$$\begin{aligned} M_p(t,t') &= \sum_{jj'} \langle\langle b_j(t) b_{j'}(t')\rangle\rangle \hat{H}_j(\vec{X}) \exp[-i\hat{H}_p(t-t')/\hbar] H_{j'}(\vec{X}) \\ \langle\langle b_j(t) b_{j'}(t')\rangle\rangle &= \sum_\beta w_\beta b_j^\beta(t) b_{j'}^\beta(t') \end{aligned} \tag{3.57}$$

These expressions are similar to the ones that appear in the literature [Kubo et al 1989, Blum 1981] and can be analyzed analogously The fluctuation and dissipation terms of the affective Hamiltonian include the average of the collective motion operators and the time correlation of pairs of them respectively The assumption of Brownian motion for the adsorbate interacting with the substrate means that the substrate DFs oscillate rapidly and irregularly on the time-scale of the adsorbate motions so that the substrate rapidly reaches temporal equilibrium. Therefore, at each time one can write

$$\langle\langle b_j(t)\rangle\rangle_t = 0 \tag{3.58}$$

and that the time-correlation function (TCF) is independent of the time t

$$\langle\langle b_j(t) b_{j'}(t')\rangle\rangle_t = \langle\langle b_j(0) b_{j'}(\tau)\rangle\rangle_t \tag{3.59}$$

where $\tau = t' - t$ and the subindex t indicates that the average is over a temporary equilibrium distribution

This time correlation function may be analyzed into its Fourier components to discover how the secondary DF frequency range will shape the time correlation

The simplest assumption consistent with chaotic motion is that all the Fourier components contribute the same amount. One then finds

$$\begin{aligned} \langle\langle b_j(t) b_{j'}(\tau)\rangle\rangle_t &= \int_{-\infty}^{\infty} d\omega \, \exp(i\omega\tau) C_{jj'}(\omega, t) \\ &= C_{jj'}(0,t) 2\pi\delta(\tau) \\ \tilde{C}_{jj'}(0, t) &= (2\pi)^{-1} \int_{-\infty}^{\infty} d\tau \langle\langle b_j(t) b_{j'}(\tau)\rangle\rangle_t \end{aligned} \tag{3.60}$$

Here the Fourier transform depends only parametrically on the time t. These results give $\hat{R}_p = 0$ and $\hat{M}_p(t, t') = \delta(t - t')\hbar\hat{W}_p(t)/2$ with

$$\hat{W}_p = 4\pi\hbar^{-1} \sum_{jj'} C_{jj'}(0, t) H_j(\vec{X}) H_{j'}(\vec{X}) \tag{3.61}$$

This expression can also be rewritten in terms of primary electronic states, using

$$H_j(\vec{X}) = \sum_{I=1}^{N} \sum_{J=1}^{N} |\psi_I^s(\vec{X})\rangle H_j^{IJ}(\vec{X}) \langle\psi_J^s(\vec{X})| \tag{3.62}$$

to obtain

$$\begin{aligned} \hat{W}_p &= \sum_{IJ} W_{IJ}(\vec{X}, t) |\psi_I^s(\vec{X})\rangle\langle\psi_J^s(\vec{X})| \\ W_{IJ}(\vec{X}, t) &= 4\pi\hbar^{-1} \sum_{jj'} C_{jj'}(0, t) \sum_{K} H_j^{IK}(\vec{X}) H_{j'}^{KJ}(\vec{X}) \end{aligned} \tag{3.63}$$

having used the orthonormality of the primary electronic states, i.e. $\langle\psi_J^s|\psi_I^s\rangle = \delta_{IJ}$. The dissipation potential is thus given in terms of the integrated time-correlation functions of the substrate. The triple sum in the dissipation potential indicates that it requires a product of two couplings $I \to K \to J$ with a common intermediate state. The derived expressions are more general than the Langevin form of the dissipation term: an instantaneous dissipation is also found, but it refers to the temporary thermal equilibrium instead of the stable equilibrium reached after long times This makes it possible to deal with substrates described by a time-dependent temperature in accordance with the recent experimental results [Cavanagh et al 1993, Germer et al 1993, Prybyla et al 1990 and 1992] More detailed expressions for the dissipation potential can be found from the derivations for phonon and e-h excitations

For phonons, from the corresponding section using the linear SCF potential,

$$\hat{h}_{\nu}^{(\beta)} = \sum_{I\,J} |\psi_I^{\rho}(\vec{X})\rangle h_{IJ}^{(\beta)}(\vec{X}\ t)\langle\psi_J^{\rho}(\vec{X})| \tag{3 64}$$

$$h_{IJ}^{\beta}(\vec{X},t) = \sum_{\nu} H_{\nu}^{IJ}(\vec{X}) q_{\nu}^{\beta}(t) \tag{3 65}$$

This gives

$$\begin{gathered}\hat{W}_{p}^{\nu} = \sum_{I\,J} W_{IJ}^{\nu}(\vec{X},t) |\psi_I^{\rho}\left(\vec{X}\right)\rangle\langle\psi_J^{\rho}\left(\vec{X}\right)| \\ W_{IJ}^{\nu}(\vec{X},t) = 4\pi\hbar^{-1} \sum_{\mu,\nu} [\sum_{K} H_{\mu}^{IK}(\vec{X}) H_{\nu}^{KJ}(\vec{X})] \int d\tau\ \langle\langle q_{\mu}(t) q_{\nu}(\tau)\rangle\rangle_t\end{gathered} \tag{3 66}$$

so that the strength of the dissipation is found from the integrated time-correlation of the vibrational displacement averages $q_{\nu}(t)$ These can be replaced [eqn (3 25)] to obtain

$$\begin{gathered}\int_{-\infty}^{\infty} d\tau\ \langle\langle q_{\mu}(t) q_{\nu}(\tau)\rangle\rangle_t = \langle\langle q_{\mu}(t) q_{\nu}(t)\rangle\rangle_t \int_{-\infty}^{\infty} d\tau\ g_{\nu}(\tau) \\ +\langle\langle q_{\mu}(t) p_{\nu}(t)\rangle\rangle_t \omega_{\nu}^{-1} \int_{-\infty}^{\infty} d\tau\ f_{\nu}(\tau)\end{gathered} \tag{3 67}$$

From the section on phonon dynamics, it is also apparent that the average over all times appearing in the dissipation term would give zero if the effect of the adsorbate on the secondary region were neglected because $q_{\nu}(t)$ would then be combinations of sine and cosine functions and their integrals would vanish except for a vanishing lattice frequency. The only terms in $q_p(t)$ which contribute to the instantaneous dissipation come from the self-consistent coupling that has been introduced which alters the oscillations in the secondary DFs. Dissipation through lattice vibrations would be absent were it not for the self-consistent treatment.

For electron-hole excitations, using results from the corresponding section

$$h_p^{(\beta)} = \sum_{IJ} |\psi_I^\beta(\vec{X})\rangle h_{IJ}^{(\beta)}\left(\vec{X},t\right)\langle\psi_J^\beta(\vec{X})| \tag{3.68}$$

$$h_{IJ}^{(\beta)}\left(\vec{X},t\right) = \sum_{\lambda}\sum_{\lambda'}\gamma^{\beta}_{\lambda,\lambda'}(t)H^{I,J}_{\lambda,\lambda'}(\vec{X}) \tag{3.69}$$

This gives, in analogy with the phonon case

$$\begin{gathered} W_p^{eh} = \sum_{IJ} W_{IJ}^{eh}(\vec{X},t)|\psi_I^\beta(\vec{X})\rangle\langle\psi_J^\beta(\vec{X})| \\ W_{IJ}^{eh}(\vec{X},t) = 4\pi\hbar^{-1}\sum_{\lambda\lambda'\lambda''\lambda'''} C_{\lambda\lambda',\lambda''\lambda'''}(0,t)\sum_{k} H^{I,k}_{\lambda\lambda'}(\vec{X})H^{k,J}_{\lambda''\lambda'''}(\vec{X}) \\ C_{\lambda\lambda',\lambda''\lambda'''}(0,t) = \int_{-\infty}^{\infty} d\tau\,\langle\langle\gamma_{\lambda\lambda'}(t)\gamma_{\lambda''\lambda'''}(\tau)\rangle\rangle_t \end{gathered} \tag{3.70}$$

Hence, the dissipation potential depends on the integrated TCF of electron density fluctuations which can relate to intraband or interband transitions. For both intraband and interband dissipation the TCFs appear integrated over all times in the instantaneous dissipation term. This term would vanish identically if the effect of the adsorbate on the secondary DFs were ignored, because the density fluctuations would then oscillate harmonically. The self-consistent field treatment of this work gives a nonzero result because it includes in the secondary effective Hamiltonian a term describing electron state couplings due to the presence of the adsorbate.

CHAPTER 4

TIME EVOLUTION OF THE PRIMARY DEGREES OF FREEDOM

TD Schrödinger Equation for the Primary DFs

This chapter studies the primary DFs quantum dynamics of the Ni(100)(ads)CO system. It is governed by the time dependent Schrödinger equation (TDSE) with the primary DF effective Hamiltonian derived from the SCF treatment of Chapter 2,

$$i\frac{\partial}{\partial t}|\psi^{p}(t)\rangle = \hat{F}_{p}|\psi^{p}(t)\rangle \qquad (4.1)$$

where $\hbar = 1$ here and henceforth. The wavefunction $\psi^{p}(t)$ is a function of all the primary coordinates and time. It fully describes the dynamics of the adsorbate in the presence of the substrate, which is modeled as a dissipative medium. The primary effective Hamiltonian from Chapter 2, is

$$F_{p} = -\left(\frac{1}{2M_{CO}}\frac{\partial^{2}}{\partial R^{2}} + \frac{1}{2\mu_{CO}}\frac{\partial^{2}}{\partial r^{2}}\right) + \bar{V}(R,r) - \frac{i}{2}W(R,r) \qquad (4.2)$$

where R is the distance between the CO center of mass and the surface, and r is the C-O distance. Due to the mass difference between electrons and atomic nuclei the time scales for electronic motion are much slower than those of the nuclear motion, so it is reasonable, in the spirit of the Born Oppenheimer approximation, to separate the nuclear kinetic energy (the first two terms in brackets) from the rest of the Hamiltonian — the complex potential energy. The equation (4.2) implies that the imaginary potential depends only on the primary coordinates and not their conjugate momenta. This is justified by the physical meaning attributed to the imaginary potentials — broadening of the discrete quantum energy levels of the primary DFs. The form of the imaginary potential was derived in detail in Chapter 3 for the secondary DFs describing vibrational and electronic excitations of the substrate, and the above assumption is confirmed.

It is suitable to choose a basis of electronic states (parametrically dependent upon nuclear variables) in which to expand the primary wavefunction; the coefficients of expansion are then functions of both nuclear variables and time

$$|\psi^p(t)\rangle = \sum_{J=1}^{N} \psi_J^n(R,r,t)|\psi_J^e(R,r)\rangle \qquad (4.3)$$

and the primary effective Hamiltonian is given by

$$\hat{F}_p = \sum_{IJ} |\psi_I^e(R,r)\rangle(\hat{K}_{IJ} + \hat{V}_{IJ} - i\hat{W}_{IJ}/2)\langle\psi_J^e(R,r)| \qquad (4.4)$$

where each K_{IJ} is a matrix element of the primary kinetic energy operator on nuclear variables and $\hat{V}_{IJ} - i\hat{W}_{IJ}/2$ is a matrix element of the complex potential energy function of the nuclear variables. The electronic states $|\psi_J^e(R,r)\rangle$ for the case of Ni(ads)CO are the molecular orbitals (MOs) of the adsorbate–substrate complex, and not of the isolated CO.

The expansion (4.3) is then introduced into the TDSE, so it can be written in the matrix form

$$i\frac{\partial}{\partial t}\psi^n(t) = \left[\mathbf{K} + \mathbf{V}(R,r) - \frac{i}{2}\mathbf{W}(R,r)\right]\psi^n(t) \qquad (4.5)$$

where $\hat{\mathbf{K}}$ is the kinetic energy operator on nuclear variables, an N by N matrix, $\mathbf{V}$ and $\mathbf{W}$ are the N by N matrices of the complex potential energy, and $\psi^n(t)$ is an N by 1 column matrix.

The elements of the kinetic energy matrix are

$$(\mathbf{K})_{I,J} = \frac{1}{2M_{CO}}\left[-i\delta_{I,J}\frac{\partial}{\partial R} - i\langle\psi_I^e(R,r)|\frac{\partial}{\partial R}|\psi_J^e(R,r)\rangle\right]^2 + \\ +\frac{1}{2\mu_{CO}}\left[-i\delta_{I,J}\frac{\partial}{\partial r} - i\langle\psi_I^e(R,r)|\frac{\partial}{\partial r}|\psi_J^e(R,r)\rangle\right]^2 \qquad (4.6)$$

where the second term in each square bracket represents the momentum coupling between the electronic basis states.

The elements of the real potential energy matrix are given by

$$(\mathbf{V}(R,r))_{I,J} = \langle\psi_I^e(R,r)|\hat{V}(R,r)|\psi_J^e(R,r)\rangle \qquad (4.7)$$

and they represent all Coulomb-type interactions between the electronic basis states. Finally, the imaginary potential matrix elements are given by

$$(\mathbf{W}(R,r))_{I,J} = \langle\psi_I^e(R,r)|W(R,r)|\psi_J^e(R,r)\rangle \qquad (4.8)$$

Again, as in Chapter 2, the above formalism must be expanded to include interaction with light. Since the radiation field is treated quantum-mechanically [Louisell 1973, Srivastava and Micha I 1991], it is convenient to define a new electronic basis as a direct product of the basis of adsorbate-substrate electronic orbitals and the photon number wavefunctions labelled as $|n_k\rangle$, so that

$$|J, n_k\rangle = |\psi_J^e(R,r)\rangle \otimes |n_k\rangle \qquad (4.9)$$

where n_k is the photon number. This basis constitutes a so-called electron field representation [Lin and George 1980]. This study of the Ni(001)(ads)CO system interacting with light includes electronic excitations and one photon processes, so the primary basis states are $|g, 1_k\rangle$ (ground electronic state of the adsorbate-substrate complex with one photon present) and $|e, 0_k\rangle$ (excited electronic states with no photons). In this basis, the matrix of the radiation field Hamiltonian is

$$\mathrm{H}_L = \begin{bmatrix} \omega_R & 0 \\ 0 & 0 \end{bmatrix} \tag{4 10}$$

while the system-field coupling Hamiltonian matrix is

$$\mathbf{H}_{pL} = \begin{bmatrix} 0 & i\sqrt{\omega_R/2\varepsilon_0}D(R,r) \\ -i\sqrt{\omega_R/2\varepsilon_0}D(R\ r) & 0 \end{bmatrix} \tag{4 11}$$

where $D(R\ r)$ is the transition dipole moment

The next task is to find a suitable basis set of electronic states to evaluate these matrices i e to choose an electronic representation There is an infinite number of possibilities but the choice is made to facilitate the numerical solution of the problem.

Electronic Representations

Of all possible electronic representations, two are especially useful — in each of them one of the terms of the Hamiltonian matrix is diagonal The first one eliminates the electronic coupling between the different basis states through the potential energy matrix and it is called the adiabatic representation [Smith 1969 Baer 1975, Olson and Micha 1982, Heather and Metiu 1987 Fernández and Micha 1991, Cohen and Micha 1992] Hence

$$[\mathrm{V}^{(a)}(R\ r)]_{I\ J} = \left[V_I^{(a)}(R,r)\right]\delta_{I,J} \tag{4 12}$$

The other possibility is the representation in which there is no momentum coupling between different electronic basis states and is called the strictly diabatic representation One writes

$$\mathrm{K}^{(d)} = -\left(\frac{1}{2M_{CO}}\frac{\partial^2}{\partial R^2} + \frac{1}{2\mu_{CO}}\frac{\partial^2}{\partial r^2}\right)\mathrm{I} \tag{4 13}$$

where M_{CO} is the total mass of CO, μ_{CO} is its reduced mass and I is the identity matrix. In this representation, the matrices of the complex potential energy are nondiagonal and, for a particular case of two electronic states, their explicit forms are

$$\mathbf{V}^{(d)} = \begin{bmatrix} V_{11}(R,r) & V_{12}(R,r) \\ V_{21}(R,r) & V_{22}(R,r) \end{bmatrix} \tag{4.14}$$

and

$$\mathbf{W}^{(d)} = \begin{bmatrix} W_{11}(R,r) & W_{12}(R,r) \\ W_{21}(R,r) & W_{22}(R,r) \end{bmatrix} \tag{4.15}$$

The physical model in this study is developed in the diabatic representation, the momentum couplings, with a form usually unknown, are replaced by functions of coordinates large only in the vicinity of potential crossings or avoided crossings; the resulting electronic couplings between different basis states contribute to both the real and the imaginary part of the primary DFs Hamiltonian. These couplings have two physical causes: interaction between the primary and secondary DFs charge distributions (predominantly the adsorbate dipole moment with the image dipole in the substrate) and the momentum couplings between the primary electronic states.

The elements of the real and imaginary potential matrices (4.14) and (4.15) are all functions of the primary coordinates only, therefore both $\mathbf{V}^{(d)}$ and $\mathbf{W}^{(d)}$ are real and symmetric matrices (so that $V_{12} = V_{21}$ and similarly for the imaginary part). This means that they can be diagonalized by orthogonal transformations, as a special case of diagonalization of Hermitian matrices by unitary transformations [Arfken 1985]. An important point here is that these unitary transformations are different, which will have to be taken into account later when the primary

DF time evolution operator is constructed. Also, they will depend on the initial conditions of propagation, i.e. on whether $\mathbf{H}_L$ and $\mathbf{H}_{pL}$ should be included; if so the imaginary part of the Hamiltonian matrix becomes a sum $-i\mathbf{W}^{(d)}/2+\mathbf{H}_{pL}$.

For the real part of the potential, the diagonalization of $\mathbf{V}^{(d)}$ is in fact the transformation into the adiabatic representation, as defined for real potentials [Smith 1979, Baer 1975, Olson and Micha 1982]; it is given by

$$\mathbf{V}^{(a)}(R,r) = \mathbf{L}_\mathbf{V} \cdot \mathbf{V}^{(d)}(R,r) \cdot \mathbf{L}_\mathbf{V}^\dagger \tag{4.16}$$

where the transformation matrix $\mathbf{L}_\mathbf{V}$ is an element of the SO(N) algebra [Fernández and Micha 1991] (in this particular case N=2), and can be parametrized with a rotation angle that is a function of primary coordinates,

$$\eta(R,r) = \frac{1}{2}\arctan\left[\frac{2V_{12}(R,r)}{V_{11}(R,r)-V_{22}(R,r)}\right] \tag{4.17}$$

Then the transformation matrix $\mathbf{L}_\mathbf{V}$ can be written as

$$\mathbf{L}_\mathbf{V} = \begin{bmatrix} \cos\eta(R,r) & \sin\eta(R,r) \\ -\sin\eta(R,r) & \cos\eta(R,r) \end{bmatrix} \tag{4.18}$$

Now, an analogous transformation is defined for the imaginary potential matrix if the interaction with light is omitted; it is defined by

$$\mathbf{W}_\mathbf{D}(R,r) = \mathbf{L}_\mathbf{W} \cdot \mathbf{W}^{(d)}(R,r) \cdot \mathbf{L}_\mathbf{W}^\dagger \tag{4.19}$$

where, as before,

$$\mathbf{L}_\mathbf{W} = \begin{bmatrix} \cos\zeta(R,r) & \sin\zeta(R,r) \\ -\sin\zeta(R,r) & \cos\zeta(R,r) \end{bmatrix} \tag{4.20}$$

and

$$\zeta(R,r) = \frac{1}{2}\arctan\left[\frac{2W_{12}(R,r)}{W_{11}(R,r)-W_{22}(R,r)}\right] \tag{4.21}$$

It must be stressed here that the diagonalization of the imaginary potential operator does not generate a representation in the physical sense, as it does not eliminate any physical coupling, but is merely a convenient mathematical procedure that will be used in the construction of the primary DF time evolution operator.

The physical model of this study is constructed in the diabatic electronic representation: the momentum couplings in the adiabatic representation, which are large only near potential crossings or avoided crossings, are replaced by smooth coupling functions of coordinates. In the diabatic representation obtained from physical considerations, the resulting electronic couplings between basis states contribute to both the real and the imaginary part of the coupling Hamiltonian between primary and secondary DFs. When the couplings are instead available from calculations for surfaces or clusters in the adiabatic representation (Head–Gordon and Tully 1992), the diabatic matrix elements follow by the above transformation.

Time Evolution Operator with the Split Operator Scheme

The formal solution to the TD Schrödinger equation for the primary DFs can be written immediately

$$|\psi^p(t+\Delta t)\rangle = \exp\left(-iF_p\Delta t\right)|\psi^p(t)\rangle \qquad (4.22)$$

or in matrix form

$$\psi^p(t+\Delta t) = \exp\left[-i\Delta t\left(\mathbf{K}+\mathbf{V}-\frac{i}{2}\mathbf{W}\right)\right]\psi^p(t) \qquad (4.23)$$

The time evolution operator is therefore an exponential of a sum of two operator terms — kinetic and potential, and the complex potential term is a sum of two terms itself For any two operators $\hat{A}$ and $\hat{B}$ the exponential of their sum can be expressed approximately as the Weyl s formula

$$\exp\left(A+B\right) = \exp\left(\hat{A}\right)\exp\left(\hat{B}\right)\exp\left(-\frac{1}{2}\left[\hat{A},\hat{B}\right]\right) + h.o.t \qquad (4.24)$$

This expression comes from the Magnus expansion [Magnus 1954] for the product of two exponentials of operators, truncated at the first order correction It is the basic idea of the so called split operator scheme [Feit, Fleck and Steiger 1982, Leforestier et al 1991] where the time evolution is executed first by half a step with the potential propagator then by a full step with the kinetic propagator, and finally again by half a step with the potential propagator As a consequence the residual error is quadratic in the time step, rather than linear as it would be by simply approximating the exponential of the sum as the product of exponentials. To account for the complex potentials that appear the same idea will be applied on the potential propagator itself

Taking advantage of the relatively simple way of diagonalizing the potential and kinetic energy matrices for a small electronic basis (N=2) the solution to the TD Schrödinger equation can be written with the split operator scheme, such that all three exponents in the time evolution operators are diagonal in the respective bases of electronic states The solution for real potentials reads [Fernández and Macha 1991]

$$\begin{aligned}\psi^{a}(t+\Delta t) = \mathrm{L}_{\mathrm{V}}^{\dagger}\ \mathrm{U}_{\mathrm{V}}^{(a)}(\Delta t/2)\ \ \mathrm{L}_{\mathrm{V}}\ \ \mathrm{U}_{\mathrm{K}}^{(d)}(\Delta t)\\ \mathrm{L}_{\mathrm{V}}^{\dagger}\ \ \mathrm{U}_{\mathrm{el}}^{(a)}(\Delta t/2)\ \ \mathrm{L}_{\mathrm{V}}\ \ \psi^{a}(t)\end{aligned} \qquad (4.25)$$

where

$$\mathrm{U}_{\mathrm{V}}^{(a)}(\Delta t/2) = \exp\left(-\imath\Delta t\,\mathrm{V}^{(a)}/2\right) \qquad (4.26)$$

is the potential energy propagator and

$$\mathrm{U}_{\mathrm{K}}^{(d)}(\Delta t) = \exp\left(-i\Delta t\mathrm{K}^{(d)}\right) \qquad (4.27)$$

is the kinetic energy propagator.

Starting from the equation (4.23), and making use of the associativity of matrix addition, i.e. $\mathrm{H}^{(d)} = \left(\mathrm{K}^{(d)} + \mathrm{V}^{(d)}\right) - i\mathrm{W}^{(d)}/2$, the imaginary potential may be split first and then the real potential and the kinetic terms may be split inside of it. The result for the primary DFs' wavepacket propagation in that case becomes a generalization of the time evolution expression (4.25),

$$\begin{aligned}\psi^{n}(t+\Delta t) = {} & [\mathrm{L}_{\mathrm{W}}^{\dagger}\ \ \mathrm{U}_{\mathrm{WD}}(\Delta t/2)\ \ \mathrm{L}_{\mathrm{W}}] \\ & [\mathrm{L}_{\mathrm{V}}^{\dagger}\ \ \mathrm{U}_{\mathrm{V}}^{(d)}(\Delta t/2)\ \ \mathrm{L}_{\mathrm{V}}]\ \ \mathrm{U}_{\mathrm{K}}^{(d)}(\Delta t) \\ & [\mathrm{L}_{\mathrm{V}}^{\dagger}\ \ \mathrm{U}_{\mathrm{V}}^{(d)}(\Delta t/2)\ \ \mathrm{L}_{\mathrm{V}}] \\ & [\mathrm{L}_{\mathrm{W}}^{\dagger}\ \ \mathrm{U}_{\mathrm{WD}}(\Delta t/2)\ \ \mathrm{L}_{\mathrm{W}}]\ \ \psi^{n}(t)\end{aligned} \qquad (4.28)$$

where the imaginary potential propagator is given by

$$\mathrm{U}_{\mathrm{WD}}(\Delta t/2) = \exp\{-\Delta t\mathrm{W}_{\mathrm{D}}/4) \qquad (4.29)$$

where W_{D} is the diagonalized imaginary potential matrix, and the other two remain the same as before.

The expression (4.28) for the time evolution over coupled complex potential energy surfaces can be called the "double split operator scheme", as the original split operator scheme [Feit, Fleck and Steiger 1982] is employed on the whole propagator to separate first the imaginary potential contribution, and then again on the primary Hamiltonian propagator to separate its kinetic and real potential contributions.

CHAPTER 5
POTENTIAL ENERGY FUNCTIONS AND THEIR COUPLING FOR PRIMARY DEGREES OF FREEDOM

Primary DF Potential Energy Surfaces and their Couplings

The physical model for photodesorption of diatomic molecules from transition metal surfaces was introduced and developed in the previous chapters. Now it must be specified for the electronic potential energy surfaces (PESs) as functions of primary DFs; they are later used for studying the quantum molecular dynamics of the Ni(001)(ads)CO system.

The ground state PES must describe a bound state of the adsorbate on the substrate surface, therefore it must have a minimum for some equilibrium distance R_g between the adsorbate's center of mass and the adsorption site. In the simplest case [Menzel and Gomer 1964, Redhead 1964, Hermann and Bagus 1977] the whole system is treated as a quasi-diatomic and the ground state PES may be defined e.g. as a Morse potential in the distance R between the surface and the center of mass of the adsorbate that is treated effectively as an atom

$$U_g^M(R) = V_g\left[e^{-2a_g(R-R_g)} - 2e^{-a_g(R-R_g)}\right] \qquad (5.1)$$

The form of the excited electronic state is expected to vary for different systems. It may be a bound state, so it can also be described by a Morse potential with a constant displacement to account for the asymptotic energy difference

$$U_e^M(R) = V_e\left[e^{-2a_e(R-R_e)} - 2e^{-a_e(R-R_e)}\right] + \Delta V_e \qquad (5.2)$$

In this case the desorption is possible through a DIMET process discussed in Chapter 2, an example being the Pt(ads)NO system [Gadzuk 1991, Misewich et al. 1992]. On the other hand, the excited electronic state may be repulsive in R, as assumed by the MGR model, so one may write the MGR-type repulsive potential in the reaction coordinate R as

$$U_e^{MGR}(R) = V_e e^{-\alpha_e R} + \Delta V_e \tag{5.3}$$

Such systems, Ni(ads)CO being one of them, evolve over the excited state PES after a Franck-Condon type transition from the ground state and thus directly desorb from the substrate.

Clearly, the potential (5.1) does not include any internal properties of the adsorbate. For diatomics, it is reasonable to expect that the internal vibration will be excited in the desorption dynamics; however, the typical diatomic bonds are much tighter than the typical chemisorption bonds, for example, the desorption energies for CO adsorbed relative to the Ni surfaces [Heskett et al. 1985] are around 1.3 eV, compared to C–O dissociation energy of 11.3 eV [Herzberg 1960]. This means that the dissociation of the adsorbate is unlikely for the processes of interest in this work (light wavelength of approx. 250 nm equivalent to approximately 5 eV energy — substantially less then the dissociation energy of CO), so the internal vibration of the adsorbate can be described as a harmonic potential well in the diatomic distance r around the equilibrium value r_g

$$U_g^h(r) = \frac{\mu\Omega^2}{2}(r - r_g)^2 \tag{5.4}$$

A further refinement of the Menzel-Gomer-Redhead (MGR) model is achieved by taking into account the interaction of the permanent dipole moment of the adsorbate (such as CO) with the induced dipole moment that its presence creates in the substrate. It is assumed that the adsorbate permanent dipole moment can be expanded around the equilibrium internal distance, up to the linear order in r, it then becomes

$$\vec{d}_g(r) = [d_{g0} + d_{g1}(r - r_g)]\vec{n}_r \tag{5.5}$$

The aforementioned interaction is then described as the interaction of the above dipole with its image in the surface, so the potential energy is

$$U_g^d(R, r) = -\frac{[d_{g0} + d_{g1}(r - r_g)]^2}{2R^3} \tag{5.6}$$

which is just one half of the interaction of two antiparallel dipoles separated by R. The factor 1/2 comes in due to the fact that one of them is an image dipole [Jackson 1975] and therefore the energy density of that interaction is

$$w = -\frac{1}{2}\vec{P}_{ind} \cdot \vec{E}_{ex} \tag{5.7}$$

where $\vec{P}_{ind}$ is the induced polarization of the medium and $\vec{E}_{ex}$ is the external electric field.

Finally, the ground state PES is obtained by adding up the contributions (5.1), (5.4) and (5.6), so the final result is

$$\begin{aligned} V_g(R, r) = V_g^0 \left\{ e^{-2\alpha_g[R - R_g - \gamma(r - r_g)]} - 2e^{-\alpha_g[R - R_g - \gamma(r - r_g)]} \right\} \times \\ \times [1 + b_g(r - r_g)] + \\ + \frac{\mu\Omega_g^2}{2}(r - r_g)^2 - \frac{[d_{g0} + d_{g1}(r - r_g)]^2}{R^3}\left\{\frac{1}{2} + \frac{1}{2}\tanh[\delta(R - R_d)]\right\} \end{aligned} \tag{5.8}$$

where $\gamma = m_C/(m_C + m_O)$ is the mass factor that appears because of the definition of R (N_2 to CO center of mass distance, rather than the N_2-C distance).

The first term of this potential function is a Morse potential in the Ni-C distance describing a relatively weak chemisorption bond between Ni and CO, multiplied by a factor that introduces coupling of the two nuclear coordinates; the distances R_g and r_g denote the minimum of the potential. The second term of the ground state PES is a harmonic potential in r describing a strong chemical bond between C and O, allowing for vibrations but not the dissociation of the adsorbate. The third term describes the interaction between the permanent dipole moment of CO expanded up to the first order in r and its image dipole induced in the substrate; a switching function is multiplied into it to provide a cutoff at short distances.

The ground electronic state of the Ni(001)(ads)CO system has been studied thoroughly [Sung and Hoffmann 1985, Albert and Yates 1987, Zangwill 1988]; parameters for the ground state PES given by the eqn. (5.8) are presented in table 5.1, with references. The parameters of the dipole interaction and the coupling between R and r were obtained from electronic structure calculations — details are given in the final section of this chapter.

The imaginary part of the ground state potential comes from the coupling of the CO 5σ orbital with the substrate lattice vibrations and intraband electronic transitions within the Ni conduction band, as shown in Chapter 3. This coupling must vanish for large values of R, as the adsorbate remains in its ground state asymptotically. The chosen parametrization is

$$W_g(R,r) = W_g^0 \exp\left[-2\alpha_g(R - \gamma r - R_g)\right]\;\left[1 + b_g(r - r_g)\right] \qquad (5.9)$$

i.e. the functional dependence is the same as that of the repulsive term of the Morse potential in $V_g(R,r)$, with a separate strength parameter. As was shown in Chapter 3 the dissipation strength parameter W_g^0 is related to the density and charge fluctuations in the substrate, however, in this study it is left as a variable parameter in calculations.

Table 5.1 Table of parameters for the Ni(001)(ads)CO ground electronic state, from previous results

Parameter	Magnitude in atomic units	Reference
V_g (chemisorption energy)	4.78×10^{-2}	Heskett et al 1985
α_g (obtained from Ni CO stretch frequency)	1.13	Maruca et al 1990
$R_{Ni\,C_g}$ (Ni C equilibrium distance)	3.40	Andersson and Pendry 1979
$\gamma = m_C/(m_C + m_O)$	0.428	
Ω_g (C-O stretch frequency)	9.4×10^{-3}	Maruca et al 1990
r_g (C O equilibrium distance)	2.132	Herzberg 1960

In analogy with the ground electronic state, the dipole dipole term and the internal vibration harmonic potential are added to the exponentially decaying repulsive potential in R, so the complete excited state PES is given by

$$V_e(R,r) = V_e^0 \exp\left[-\alpha_e(R-\gamma r)\right]\ \left[1+b_e(r-r_e)\right] + \Delta V_e + \\ + \frac{\mu\Omega_e^2}{2}(r-r_e)^2 - \frac{\left[d_{e0}+d_{e1}(r-r_e)\right]^2}{R^3}\left\{\frac{1}{2}+\frac{1}{2}\tanh\left[\beta(R-R_d)\right]\right\} \qquad (5\ 10)$$

The first term is a repulsive exponential function in the Ni C distance, describing the antibonding between Ni and C again with coupling of the nuclear coordinates The second term is the asymptotic energy difference between the Ni conduction and lowest unoccupied bands. The last two terms are analogous to the corresponding terms in the ground state PES The parameters of the excited state PES (5 10) were obtained by fitting the results of the electronic structure calculations explained in a later section

The imaginary part of the excited state potential is again parametrized as a repulsive exponential function in the Ni C distance

$$W_e(R,r) = W_e^0 \exp\left[-\alpha_e(R-\gamma r)\right]\ \left[1+b_e(r-r_e)\right] \qquad (5\ 11)$$

Again, the dissipation strength parameter W_e^0 related to the substrate dynamics is left as a variable parameter

It is apparent that this model of adsorption does not take into account the overall rotation of the adsorbate It is assumed that its symmetry axis is perpendicular to the surface and thus no angular variable is used among the primary DFs The theoretical [Hermann and Bagus 1977] and experimental [Akimoto et al 1979] results for Ni(001)(ads)CO support this assumption

The remaining problem is to parametrize the off-diagonal or coupling terms of the potential energy matrices labelled by an index "c" Their real part represents the diabatic electronic coupling between the basis states so it can differ significantly from zero only in the regions close to crossings or avoided crossings of the PESs. These regions are expected to occur at short adsorbate-substrate distances, because of the functional form of the Morse potential. One possible form to describe such behaviour is with a cut-off function

$$V_c(R,r) = \frac{V_c^0}{2}\{1 - \tanh[\alpha_c(R - \gamma r - R_c + \gamma r_c)]\} \qquad (5.12)$$

where R_c and r_c denote the position of surface crossing.

The imaginary coupling potential $W_c(R,r)$ appears, as was deduced in Chapter 3, from the coupling of the adsorbate electronic states with the interband electronic transitions (between the conduction and upper empty bands) of the substrate. Like $W_g(R,r)$ and $W_e(R,r)$, it is expected to have a short range contribution coming from the choice of electronic representation, but in addition, there should be a longer range term from the interaction of the induced dipole moments of the adsorbate and the substrate. The proposed parametrization is

$$W_c(R,r) = \frac{W_c^0}{2}\{1 - \tanh[\alpha_c(R - \gamma r - R_c + \gamma r_c)]\} \qquad (5.13)$$

which comes from the diagonalization of **W** and is analogous to the real diabatic coupling V_c.

The real PESs (5.8) and (5.10) with diabatic coupling (5.12), as functions of the adsorbate-substrate distance R, for a fixed value of r corresponding to the ground electronic state equilibrium vibrational distance between C and O, are illustrated in figure 5.1.

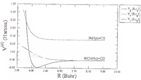

Figure 5.1 Potential energy surfaces with diabatic coupling vs. adsorbate-substrate distance R for fixed equilibrium value $r=r_g$ for the Ni(001)(ads)CO system.

Transition Dipole Moment for CO Photodesorption

By the initial assumption of this study the transition dipole moment between the adsorbed electronic state of CO and the desorbing excited state is defined as a function of primary degrees of freedom (i e adsorbate nuclear coordinates) only so that

$$D = D(R\ r) \tag{5 14}$$

The customary parametrizations for this operator in the literature [Kirby and Goldfield 1990 Pradhan et al 1991] are of polynomial type often with an attenuation factor to account for the relatively short range of interaction A more accurate parametrization was possible due to the electronic structure calculations, commented in the next section The transition dipole was found to increase almost linearly with the adsorbate substrate distance R with a gradual cutoff beyond an $R = R_{cr} = const.$ while its value is almost independent of the C O distance r again up to a cutoff at $r = r_{cr}(R)$ A good fitting was found for a function

$$\begin{aligned} D(R,r) = (D_0 + D_1 R + D_2 R^2)\{1 - \tanh[\eta(R - R_{cr})]\}\times \\ \times\{1 - \tanh[\zeta(r - r_{cr}(R))]\} \end{aligned} \tag{5 15}$$

with

$$r_{cr}(R) = r^0_{cr} + \xi\left(\frac{R^2}{R^2_{cr}} - 1\right) \tag{5 16}$$

Electronic Structure Calculations of the Region of Primary DFs

This section gives a more detailed explanation of the electronic structure calculations that were done for the NiCO molecule and for CO adsorbed on the top site of an Ni_{16} cluster, in order to gain a better insight into the CO adsorption mechanism on the Ni(001) surface and the character of the electronic transition that leads to its desorption and to obtain a reliable semiempirical parametrization for the PESs with their couplings and the transition dipole moment, to be used later in the computation of the primary DF dynamics. These calculations were done using the ZINDO software [Ridley and Zerner 1973, Zerner et al. 1980].

To calculate the ground state energy of the given molecule, as well as the effective atomic charges and electronic populations of the molecular orbitals (MOs), the ZINDO program runs an iterative Hartree-Fock (HF) type calculation for a specified geometry and total spin state. The relative positions of the C and O atoms with respect to the adsorption site Ni atom were varied around the known equilibrium values [Heskett et al. 1985], while the Ni_{10} cluster was constructed by taking into account the eight nearest neighbours and the atom underneath the adsorption site of the known FCC crystal structure of the nickel solid. The total spin state was chosen to be a singlet (no unpaired electrons) for NiCO and a triplet (two unpaired electrons) for $Ni_{10}CO$, as those choices were the closest approximations to the experimental value of the effective magnetic moment of 0.6 Bohr magnetons per atom for the nickel metal [Kittel 1957], which comes from the spin decoupling of its 3d-4s conducting band. In fact, a higher multiplicity would have been even closer for $Ni_{10}CO$, but high spin multiplicities present a difficulty for convergence of the calculations. Information on the input data for the mentioned ZINDO calculations can be found in Appendix B.

As a general trend, the HF calculations reproduced quite well the experimental equilibrium O-C and C-Ni distances [Heskett et al. 1985]; however, the computed binding energy was substantially larger than its experimental value due to the strong deformation of the MOs of CO and the adsorption site Ni atom. This deformation, in fact larger for Ni$_{13}$CO than for NiCO, is a consequence of representing an infinite solid with a small atomic cluster so the attractive forces between CO and the Ni atomic cores are not properly balanced. This problem was resolved by rescaling the computed values of energy to fit the known ground state PES [Andersson and Pendry 1979]; later, energies of the excited states were rescaled by the same factor to obtain the excited PES parametrization.

As stated before, the parameters of the dipole interaction and the coupling between R and r in the ground state PES [eqn. (5.8)] were determined by the ZINDO-HF calculations; they are given in table 5.II.

Table 5.II. Table of parameters for the dipole coupling and the R-r coupling for the Ni(001)(ads)CO ground electronic state, from electronic structure calculations.

Parameter	Magnitude in atomic units
d_{g0}	0.028
d_{g1}	0.054
b_g	0.0
R_d	4.0
δ	0.5

To compute the excited states of the molecule of interest, the ZINDO software uses configuration interaction (CI) calculations, initiated by a HF ground state, but with a changed basis set. Again, positions of nuclei and the total spin state must be specified for each run. The ZINDO CI calculations give as a result a multitude of excitations with transition energies, transition dipole moments, and oscillator strengths that are related to the probabilities of corresponding transitions. The input data for those calculations are listed in Appendix B.

The ZINDO CI calculations were done on the NiCO molecule to determine the desorbing excited state PES and the corresponding transition dipole moment. The strongest transition was detected from a linear combination of $0.30|Ni\ 3d_{x^2-y^2}\rangle - 0.95|Ni\ 3d_{xy}\rangle$ and $0.95|Ni\ 3d_{x^2-y^2}\rangle + 0.30|Ni\ 3d_{xy}\rangle$ orbitals, to the $0.88|Ni\ 4p_z\rangle - 0.37|C\ 2s\rangle$ orbital of the NiCO complex. The excited PES was then determined by adding the rescaled transition energy to the ground state value for different interatomic distances. As expected from the theoretical analysis, the "destination" orbital is antibonding between nickel and carbon so it does indeed lead to desorption, as assumed by the MGR model. The parameters of the eqs. (5.10) were then fitted to reproduce the obtained excited PES energies as functions of R and r; their values are given in table 5.III.

Table 5.III. Parameter table for the Ni(001)(ads)CO excited electronic state PES

Parameter	Magnitude in atomic units
V_e	1.44×10^{3}
α_e	2.56
ΔV_e	0.0128
r_e	2.3
Ω_e	9.25×10^{-3}
d_{e0}	0.028
d_{e1}	-0.014
b_e	0.15

The parameters of the transition dipole moment between the linear combination of $0.30|Ni\ 3d_{x^2-y^2}\rangle - 0.95|Ni\ 3d_{xy}\rangle$ and $0.95|Ni\ 3d_{x^2-y^2}\rangle + 0.30|Ni\ 3d_{xy}\rangle$

orbitals, and the $0.88|Ni\ 4p_z\rangle - 0.37|C\ 2s\rangle$ orbital of NiCO corresponding to the eqn (5.15) with (5.16) are given in table 5.IV

Table 5.IV Parameters of the photodesorption transition dipole moment for Ni(001)(ads)CO

Parameter	Magnitude in atomic units
D_0	0.07
D_1	0.01
D_2	0.38
R_{cr}	4.45
r_{cr}^0	2.14
η	0.4
ζ	5.0
ξ	0.02

CHAPTER 6
NUMERICAL ASPECTS OF TIME PROPAGATION

Methods of Time Propagation of Wavepackets with Dissipation

The time propagation of wavepackets is the most important computational aspect of this study, as the time dependent amplitudes are required for calculation of the time correlation functions used in the description of the physics of photodesorption. This propagation in fact means solving numerically the time dependent Schrödinger equation (TDSE) — several methods are known for this purpose and can be found in literature [Leforestier et al 1991, Truong et al 1991].

The problem amounts to accurate and efficient construction of the time evolution operator of the TDSE, which for the primary effective Hamiltonian $\hat{F}_p$ has the form

$$U(\Delta t) = \exp\left(-i\Delta t \hat{F}_p\right) \tag{6.1}$$

with $\hbar = 1$. This operator advances the solution of the TDSE by the given time step Δt. The Hamiltonian operator $\hat{F}_p$ has been derived in previous chapters and it has a form

$$F_p = F_p\left(\vec{X}, -i\partial/\partial\vec{X}\right) = K\left(-i\partial/\partial\vec{X}\right) + \hat{V}\left(\vec{X}\right) - iW\left(\vec{X}\right)/2 \tag{6.2}$$

The radiation field and its coupling to the system do not appear in this Hamiltonian which implies the initial conditions of the time evolution such that the light had already been absorbed by the system and the primary region is in the state $|e, 0_k\rangle$

(cf. Chapter 4) at the initial time. There are various methods of numerical time evolution with the operator (6.1) [Leforestier et al. 1991, Truong et al. 1991]; two of them will be discussed in the rest of this section.

The first one starts by defining a basis set of N_b suitable functions ϕ_n [Hamilton and Light 1986] that spans the whole space of interest (in this context N_b is the dimensionality of the basis set and not the physical dimensionality of space — number of degrees of freedom). The wavepacket $\psi^n(t)$ then becomes a column matrix with elements

$$\psi_j^n(t) = \int \phi_j^*(\vec{X})\psi^n(\vec{X})d\vec{X} \tag{6.3}$$

and the kinetic and potential energy operator become matrices with elements

$$\mathrm{K}_{jk} = -\frac{1}{2M}\int \phi_j^*(\vec{X})\frac{\partial^2}{\partial \vec{X}^2}\phi_k(\vec{X})d\vec{X} \tag{6.4}$$

and

$$\begin{aligned}\mathrm{V}_{jk} &= \int \phi_j^*(\vec{X})V(\vec{X})\phi_k(\vec{X})d\vec{X}\\ \mathrm{W}_{jk} &= \int \phi_j^*(\vec{X})W(\vec{X})\phi_k(\vec{X})d\vec{X}\end{aligned} \tag{6.5}$$

so that the Hamiltonian matrix is the sum of these three matrices

$$\mathrm{H} = \mathrm{K} + \mathrm{V} - i\mathrm{W}/2 \tag{6.6}$$

Finally, the time evolution matrix, allowing for a nonorthogonal basis, is

$$\mathrm{U}(\Delta t) = \exp\left(-i\Delta t \mathrm{S}^{-1}\mathrm{H}\right) \tag{6.7}$$

where S is the overlap matrix of the basis functions.

The advantage of the basis expansion for wavepackets and the time evolution operator is that a good choice of the basis set, according to the physical properties of the system (symmetry, etc.), allows the use of relatively few basis functions (N_b not very large) and thus relatively small matrices for the numerical procedure. However, N_b does become prohibitively large for relatively extended systems with several degrees of freedom. Also, the matrix elements of **H** are integrals that must be calculated, and **H**, as well as **S** for a non orthonormal basis, are non-diagonal matrices, so they must be diagonalized to construct the time evolution matrix.

The alternative approach is a discretization of space and subsequent evaluation of the Hamiltonian matrix elements as functional values at the given points. The space of primary DF coordinates R and r is discretized for the numerical implementation of the time evolution scheme. This is done in the simplest fashion by introducing an equidistant two-dimensional discrete grid of n (for the R direction) by m (for the r direction) points, covering the whole space of interest: the discretized variables become $R_i = R_0 + i\Delta R$ and $r_j = r_0 + j\Delta r$, where ΔR and Δr are the grid spacings in R and r, respectively. Although this is not the most economical way in terms of the total number of points necessary (cf. discrete variable representation [Light et al. 1984, Colbert and Miller 1991, Seidmann and Miller 1991]), it has an advantage of allowing for different numerical algorithms, such as fast Fourier transform (FFT) [Press et al. 1992]. The space discretization introduces a coordinate representation, so that $\langle R_i|\hat{R}|R_{i'}\rangle = i\Delta R\,\delta_{i,i'}$. An observable — operator $\hat{A}$ is said to be local if

$$\langle R_i, r_j|\hat{A}|R_{i'}, r_{j'}\rangle = [\mathrm{A}]_{ij}\,\delta_{i,i'}\,\delta_{j,j'} \tag{6.8}$$

so when it operates on a wavefunction in the space of R and r, the different components in the coordinate representation do not mix. Obviously, all operators that are functions of coordinate operators $\hat{R}$ and $\hat{r}$ are local, in particular the potential energy operators in both diabatic and adiabatic electronic representation, as well as in the "representation" of the diagonal imaginary potential. Using this property it is advantageous to use the split operator scheme defined in Chapter 4

$$\begin{aligned} \mathbf{U}^{(d)}(\Delta t) = {} & [\mathbf{M}^{\dagger}\ \mathbf{U}_{\mathbf{W}}^{(x)}(\Delta t/2)\ \mathbf{M}]\ [\mathbf{L}^{\dagger}\ \mathbf{U}_{\mathbf{V}}^{(a)}(\Delta t/2)\ \mathbf{L}] \\ & \mathbf{U}_{\mathbf{K}}^{(d)}(\Delta t)\ [\mathbf{L}^{\dagger}\ \mathbf{U}_{\mathbf{V}}^{(a)}(\Delta t/2)\ \mathbf{L}]\ [\mathbf{M}^{\dagger}\ \mathbf{U}_{\mathbf{W}}^{(x)}(\Delta t/2)\ \mathbf{M}] \end{aligned} \tag{6.9}$$

This time evolution scheme was used in all the calculations of this study.

It is obvious that the kinetic energy operator $\hat{K}$ does not satisfy the locality condition (6.8), because the second derivatives with respect to R and r must be expressed e.g. in terms of finite differences. However $\hat{K}$ is local in the momentum representation, as

$$K = \frac{1}{2M}\hat{P}^2 + \frac{1}{2\mu}\hat{p}^2 \tag{6.10}$$

where $\hat{P}$ and $\hat{p}$ are conjugate momenta to R and r, respectively. The momentum space is discretized according to $P_k = P_0 + k\Delta P$ and $p_l = p_0 + l\Delta p$, where the grid spacings are $\Delta P = 1/(n\Delta R)$ and $\Delta p = 1/(m\Delta r)$, the kinetic energy operator then becomes

$$K = \sum_{k,l} |P_k, p_l\rangle \tilde{\mathbf{K}}^{(d)}(P_k, p_l)\langle P_k, p_l| \tag{6.11}$$

where $\tilde{\mathbf{K}}^{(d)}$ is a diagonal $(n\times m)\times(n\times m)$ matrix. The kinetic energy matrix elements in the coordinate space are given by

$$\left(\mathbf{K}^{(d)}\right)_{i,j,i',j'} = \sum_{k,l} \langle R_i, r_j | P_k, p_l\rangle \tilde{\mathbf{K}}^{(d)} \langle P_k, p_l | R_{i'}, r_{j'}\rangle \tag{6.12}$$

or in matrix notation

$$\mathbf{K}^{(d)} = \mathbf{F}_T^{\dagger}\ \tilde{\mathbf{K}}^{(d)}\ \mathbf{F}_T \tag{6.13}$$

where $(\mathbf{F}_T)_{k,l,i,j} = \langle P_k, p_l | R_i, r_j \rangle$ are elements of the Fourier transformation matrix $\mathbf{F}_T$. A multidimensional FFT algorithm [Press et al. 1992] was applied in the calculations.

Using the Fourier transformation (6.13), the time evolution operator (6.9) can now be rewritten in a numerically applicable form in which all the propagation kernels are both diagonal (referring to the electronic basis) and local (referring to the discrete grid matrix representation)

$$\begin{aligned}\mathbf{U}^{(d)}(\Delta t) = [\mathbf{L}_W^\dagger\ \ \mathbf{U}_W^{(x)}(\Delta t/2)\ \ \mathbf{L}_W]\ [\mathbf{L}_V^\dagger\ \ \mathbf{U}_V^{(a)}(\Delta t/2)\ \ \mathbf{L}_V] \\ [\mathbf{F}_T^\dagger\ \ \tilde{\mathbf{U}}_K^{(d)}(\Delta t)\ \ \mathbf{F}_T] \\ [\mathbf{L}_V^\dagger\ \ \mathbf{U}_V^{(a)}(\Delta t/2)\ \ \mathbf{L}_V]\ [\mathbf{L}_W^\dagger\ \ \mathbf{U}_W^{(x)}(\Delta t/2)\ \ \mathbf{L}_W]\end{aligned} \tag{6.14}$$

where all the matrices have been defined in Chapter 4.

On the two-dimensional grid, the primary DF nuclear wavefunction becomes a function of two discrete indices, i.e.

$$\psi^n(R,r,t) = \begin{bmatrix}\psi_g^n(R,r,t) \\ \psi_e^n(R,r,t)\end{bmatrix} \rightarrow (\psi^n)_{i,j} = \begin{bmatrix}\psi_g^n(R_i,r_j) \\ \psi_e^n(R_i,r_j)\end{bmatrix}_l = \begin{bmatrix}(\psi_g^n)_{i,j} \\ (\psi_e^n)_{i,j}\end{bmatrix}_l \tag{6.15}$$

where the time dependence has been suppressed in the notation.

An alternative method for the propagation with the non-diagonal kinetic energy matrix $\mathbf{K}$ is its diagonalization via the Lanczos reduction algorithm [Lanczos 1950]. The Fourier transform method was proven better as it was more stable for rapidly varying wavepackets (i.e. it allowed for larger values of particle wavepacket momenta) and also more economical computationally (the reduced Lanczos basis in which the tridiagonal propagation kernel is diagonalized depends upon the amplitude, so it must be computed for every time step, while the FFT procedure is relatively efficient even for multidimensional grids).

Initial Conditions for Wavepacket Propagation

Initial Conditions for the Wavefunction

As stated earlier the primary DF space of CO photodesorption from the Ni(001) surface is defined in terms of two coordinates the distance between the CO center of mass and the surface R and the internal C-O distance r. This space has been discretized and the maximal allowed grid spacings are generally determined by the momentum of wavepackets that propagate over it in each direction. The initial state of the system is described by a two-component wavefunction

$$\psi^{n}(R, r\ t = 0) = \begin{bmatrix} 0 \\ \psi_{e}(R\ r\ 0) \end{bmatrix} \qquad (6\ 16)$$

This initial state means that the time evolution begins after a short light pulse has been shining on the adsorbate-substrate complex, photons have been absorbed and a transition into the excited electronic state of the adsorbate substrate complex has occurred.

The exact form of the wavepacket $\psi_e(R, r, 0)$ depends on the exact characteristics of the electronic transition. In general, it is assumed that the transition has a Franck Condon character i e that the expectation value of the two coordinates and their conjugate momenta, as well as the shape of the wavepacket remain unchanged. Therefore, if the system had originally been in its ground vibrational state in the Morse harmonic potential well of the ground electronic PES $\psi_e(R\ r, 0)$ can be approximated by a two-dimensional harmonic oscillator ground state eigenfunction — a Gaussian in both R and r, i e.

$$\psi_e(R, r\ 0) = N \exp\left[-\alpha_R^2 (R - R_0)^2\right] \exp\left[-\alpha_r^2 (r - r_0)^2\right] \qquad (6\ 17)$$

where R_0 and r_0 denote the initial position the width parameters are $\alpha_r = \sqrt{\mu_{CO}\Omega_g/\hbar}$ and α_R is obtained from the shape of the Morse potential well of the ground state PES and N is a normalization factor This is certainly true in the case of resonant absorption, when the energy of the absorbed photon is exactly equal to the energy difference between the two PESs at the initial position of the adsorbate reduced by the zero-level vibrational energy in R

If the energy of the absorbed photon is above the resonant absorption value the initial wavepacket must have an average kinetic energy equal to the excess of the photon energy, even though its average momentum must still vanish One way to construct such a wavepacket is to multiply the original packet by a phase factor $\exp(iRP)$ and then integrate over a distribution of momenta with a standard deviation such that $\langle\hat{P}^2\rangle = 2M_{CO}\hbar\Delta\omega$ where $\Delta\omega$ is the difference of the photon frequency from the resonant absorption value The resulting wavepacket has a form

$$\psi_e(R,r,0) = N\exp\left[-\left(\alpha_R^2 + M_{CO}\Delta\omega/\hbar\right)(R-R_0)^2\right]\exp\left[-\alpha_r^2(r-r_0)^2\right] \tag{6 18}$$

This wavepacket has a correct expectation value of R, P and P^2, but is deformed in the coordinate space — it becomes narrower than the original wavepacket in R This should be acceptable for the values of $\Delta\omega$ small compared to the vibrational quanta in the excited electronic state but it can lead to unphysical results when $\Delta\omega$ becomes relatively large In that case it may be expected that the CO internal vibrational levels will become populated instead of converting the whole excess of the photon energy into the kinetic energy of the desorbing species

Initial Conditions for the Dipole Amplitude

The initial conditions described above refer to the propagation of the wave function, which is suitable to study the experimental situations involving excitations by short light pulses. If, on the other hand, one wishes to study a steady state experimental situation in which the adsorbate-substrate complex interacts with a steady beam of light, the physically appropriate description is the propagation of the dipole amplitude and the above initial wavepacket must be multiplied by the transition dipole moment. In that case, the time evolution operator becomes an effective frequency operator (cf. Chapter 2) [Srivastava and Micha I 1991] — the initial energy of the system is subtracted from the primary effective Hamiltonian so that

$$\hat{U}(\Delta t) = \exp\left[-i\left(F_p - E\right)t/\hbar\right] \tag{6.19}$$

The initial wavepacket in this case must represent the initial transition dipole amplitude, defined in Chapter 2, therefore

$$\Upsilon(R, r, t=0) = \begin{bmatrix} 0 \\ D_y(R, r)\psi_e(R, r, 0) \end{bmatrix} \tag{6.20}$$

and $\psi_e(R, r, 0)$ is the initial wavefunction defined by the eqn. (6.17). In this case, there are no modifications coming from the frequency of the absorbed light. In fact, the Fourier transform with respect to time of the dipole-dipole TCF is a function of the photon frequency and it gives the probability of desorption after absorption of a photon of the given frequency.

Numerical Parameters for Time Propagation

At later times $t > 0$ the wavepacket will have an average momentum of $\langle P\rangle_t = \sum_{I=g,e} -i\langle\psi_I(t)|\partial/\partial R|\psi_I(t)\rangle / \sum_{I=g,e} \langle\psi_I(t)|\psi_I(t)\rangle$ and similar for the r direction. The maximal allowable grid spacings are then estimated by

$$\begin{aligned} \Delta R &<< 2\pi/\langle P\rangle_t \\ \Delta r &<< 2\pi/\langle p\rangle_t \end{aligned} \tag{6.21}$$

where "much less than" implies at least several grid points per unit wavelength, i.e. about an order of magnitude.

The other critical parameter of the numerical time propagation is the time step. Neglecting for the moment the potentials, the time evolution operator matrix on a grid with spacing ΔR for a free particle of mass M can be written as

$$\mathrm{U}(\Delta t) = \exp\left[-i\frac{\Delta t}{2M(\Delta R)^2}\mathbf{D}\right] \tag{6.22}$$

where $\mathbf{D}$ is a matrix of finite differences, i.e. its elements are all numbers of the order of unity and smaller. For stability of propagation, the ratio in the exponent above must be kept relatively small, as $\mathrm{U}(\Delta t)$ is multiplied into an amplitude that varies in space according to the momentum of the particle.

The time evolution method developed in this study can examine not only the desorption from surfaces, but molecular scattering problems as well. Test calculations were performed for wavepackets of initial Gaussian amplitude, modulated by a phase factor $\exp(-iP_0R)$ to reproduce the initial momentum in the molecular scattering calculations. The method was tested to reproduce the results of two model one-dimensional (fixed r) scattering problems with two coupled PESs and without dissipation [Alvarellos and Metiu 1988, Cohen and Micha 1992]

The results for average positions and electronic state populations as functions of time [Alvarellos and Metiu 1988] were well reproduced, while the results for the electronic transition probability as a function of energy were in agreement with the reference [Cohen and Micha 1992] at low energies (less than 0.4 Hartree); the high projectile momenta presented a problem in the time-dependent calculations for comparisons at the higher energies.

Table 6.1. Grid parameters for the two-dimensional wavepacket propagation, for CO photodesorption from Ni.

Quantity / Parameter	Numerical Value (tests)	Num. value (photodesorption calcs.)
Range and no. of grid points in R	10.0 a_0, 512	10.0 a_0, 256
Range and no. of grid points in r	2.0 a_0, 64	2.0 a_0, 32
Grid spacings ΔR and Δr	1.95×10^{-2} and 3.12×10^{-2} a_0	3.90×10^{-2} and 6.25×10^{-2} a_0
CO total and reduced mass	5.22×10 and 1.25×10^4 m_e	tbd
Maximal momentum	120.0 au	≤ 30 au
Maximal time step	0.05 au	0.5 au
Maximal no. of steps	100 000	10 000

The typical momenta for the photodesorption problem are smaller then the upper limit that was tested (for example, a CO molecule with momentum of 30 au has the kinetic energy of approx. 0.25 eV) so the calculations could be performed with larger time steps, as well as with fewer grid points in each direction table 6 1 gives the numerical propagation parameters in both the preliminary test calculations and the actual wavepacket propagation used in calculations of the CO photodesorption from nickel

Algorithm for the Numerical Time Propagation

The numerical propagation of wavepackets used in the calculations of the CO photodesorption from the Ni(001) surface was executed with a Fortran 77 program "cphe2d f" and the corresponding subroutines the flow diagram of this algorithm is given in Appendix C The algorithm propagates a two dimensional wavepacket, given as a two index array by the eqn (6 15) with a time evolution operator (6 14) constructed from a Hamiltonian operator with two coupled complex potential energy surfaces by means of a split operator scheme modified to include the dissipation

The algorithm begins by the input of data, separated in two subroutines that read in the data from two separate input files The first one called "rawh2d f", reads in the data for the initial wavefunction given by the eqn (6 17) and the transition dipole moment with a functional form discussed in Chapter 5 The second one named "lcpt2d f" reads in the data for the complex PESs and their couplings all defined in Chapter 5 The program then proceeds by constructing the initial wavepacket (subroutine "inho2d f") and, if the dipole-dipole TCF is to be calculated, the initial dipole amplitude (subroutine "dpam2d f") and also the complex PESs with couplings (subroutine "cpes2d f") Evidently this structure assures a great flexibility in the use of the program as different initial conditions or potential energy functions can be obtained by merely modifying the corresponding subroutines, without changing the main program. Before starting the time propagation, the program computes the initial values of the time dependent properties such as the expectation values of coordinate operators $\hat{R}$ and $\hat{r}$ (subroutine "cent2d.f") and the TCFs — autocorrelation function or dipole-dipole TCF (subroutine "acrf2d.f").

The time evolution in this algorithm is sequential in time steps using the modified split operator scheme (6.14) to advance by one time step and calculating the time dependent properties at each time step until reaching the given final time. The time advancement is executed as a sequence of matrix multiplications given by (6.14) with overwriting of the wavepacket after each multiplication, for instance, operating with the imaginary potential propagator is done as a sequence

$$
\begin{gathered}
\chi(t) = \mathbf{L_W}\ \psi^{(d)}(t) \\
\psi^{(d)}(t) = \chi(t) \\
\chi(t, \Delta t) = \mathbf{U_{WD}}(\Delta t/2)\ \psi^{(d)}(t) \\
\psi^{(d)}(t, \Delta t) = \chi(t, \Delta t) \\
\chi(t, \Delta t) = \mathbf{L}_\mathbf{W}^\dagger\ \psi^{(d)}(t, \Delta t) \\
\psi^{(d)}(t, \Delta t) = \chi(t, \Delta t)
\end{gathered}
\qquad (6.23)
$$

using subroutines "repi2d.f" for multiplications with L_W and its adjoint, and "adcp2d.f" for multiplication with the propagator $\mathbf{U_{WD}}(\Delta t/2)$. An analogous procedure is used to advance via the real potential propagator using subroutines "repr2d.f" and "adpo2d.f". The time advancement by the kinetic energy propagator is done with a subroutine "adft2d.f" which arranges the input wavepacket into a one dimensional array suitable for the fast Fourier transform (FFT) algorithm, takes an FFT into the momentum space using the well known "fourn.f" routine

[Press et al. 1992] advances by a step Δt in the momentum space, takes the inverse FFT back into the coordinate space and rearranges the output wavepacket into a two dimensional array, overwriting the input array.

The output of the time evolution program consists of the time dependent properties — expectation values of the primary coordinates, TCFs and relative populations of the two electronic states (normalized to unity at each time step; the actual populations, obtained as absolute value squares of each wavefunction component at each time, go asymptotically to very small limits due to the dissipation), as well as the input files to obtain the two dimensional plots of the PESs and their couplings, the transition dipole moment between the electronic basis states, and the propagating amplitudes as they evolve over time.

The time propagation algorithm described in this section achieves good efficiency in both computational time and memory occupation. Although the complex PESs and their couplings are stored as two dimensional arrays, they need not be generated at each time step of the propagation — this, though increasing the necessary memory, considerably accelerates the computation. To illustrate the performance, it is worth noting that one photodesorption calculation with parameters from the third column of the table 6.1, executed on an IBM RS/6000–580 server machine, takes about 106 minutes of CPU time, occupying approximately 1.7 Mb of memory.

CHAPTER 7
RESULTS OF CALCULATIONS AND DISCUSSION

Model Calculations for Dissipative Potential Parameters

This section addresses the parametrization of the dissipative imaginary potentials that come from the SCF treatment of the adsorbate substrate coupling This problem can be related to the calculated finite lifetimes of the CO vibrational states [Persson and Persson 1980 Head Gordon and Tully 1992] when adsorbed on metal surfaces The results suggest that the lifetimes of the C O stretch vibrations must be of the order of 1 ps, while the lifetimes of the frustrated translation mode (C-Ni stretch) are of the order of 10 to 100 ps To model this system a simplified ground state complex PES is defined by

$$\begin{aligned} U_g(R\ r) = {} & \frac{M\Omega_{ft}^2}{2}(R-R_g)^2 + \frac{\mu\Omega_g^2}{2}(r-r_g)^2 - \\ & -i\frac{W_g}{2}\exp\left[-2\alpha_g(R-R_g)\right] \end{aligned} \qquad (7\ 1)$$

where the frustrated translation frequency Ω_{ft} is obtained by expanding the ground state Morse potential, given by the eqn (5 1) around its minimum No coupling of motions in R and r was included because it was found to be small (cf Chapter 5)

The harmonic oscillator eigenfunctions in two dimensions with different quantum numbers (combinations of 0 1 and 2) were then propagated with the potential (7 1) in order to test the computer program for propagation and to obtain an estimate on the dissipative potential strength in relation to the lifetime The autocorrelation function defined in Chapter 2 was calculated for each case In the absence of dissipation, its absolute value square is equal to one at all times which confirmed that the propagation algorithm contained no spurious couplings between the two primary coordinates. An example — the ground vibrational state (0 0) — for four different values of the imaginary potential strength, is shown in figure 7.1.

Assuming an exponential decay of a given vibrational state, the lifetime can be expressed as

$$\tau^{-1} = \lim_{t\to\infty} \left\{ -\frac{d}{dt} \ln \left[|C(t)|^2 \right] \right\} \tag{7.2}$$

where in practice the limit is evaluated for the final time of the propagation, $t_f = 1.0 \times 10^3$ au. Results obtained for the ground harmonic state (0 0) are presented in table 7.1.

Table 7.1. Lifetime of ground vibrational state of Ni(ads)CO for different values of the imaginary potential strength W_0.

W_0 (10^{-3} E_h)	$\mid C(t_f) \mid^2$	τ (ps)
0.00	1.0	∞
0.02	0.97980	1.0717
0.05	0.95031	0.4291
0.10	0.90317	0.2147
0.20	0.81598	0.1071
0.50	0.60281	0.0430
1.00	0.36609	0.0218

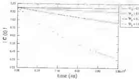

Figure 7.1 Autocorrelation function vs. time for a 2D harmonic oscillator ground state for different values of the dissipation strength parameter

These results clearly show that for the given model the lifetime of vibrational states is inverse proportional to the strength of the dissipative imaginary potential. Similar results were obtained for the excited vibrational states of the system. They indicate that the imaginary part of the primary ground electronic state PES must have a magnitude of the order of 10^{-5} au in order to reproduce the known vibrational lifetimes. For the case of Ni(001)(ads)CO, however, the electronic excitations are expected to be the primary way of energy dissipation [Newns, Heinz and Misewich 1991], so the parameters W^0_g and W^0_e are expected to be larger; the initial guess for the time propagation in this work was $W^0_g = 8.78 \times 10^{-4}$ au and $W^0_e = 1.14 \times 10^{-3}$ au. The magnitude of the imaginary part of the diabatic coupling was initially set at $W^0_c = 1.23 \times 10^{-3}$ au.

The calculations that follow were done for two different initial conditions corresponding to an excitation by a light pulse or by a steady light beam, as indicated in Chapter 6.

Calculations of CO Photodesorption: Varying the Incident Light Wavelength

The theory of photodesorption dynamics developed in this study, with the initial conditions specified in Chapter 6, assumes up to this point that the electronic transition in the adsorbate-substrate complex leading to the desorption was caused by a resonant absorption of a photon, i.e., that its frequency was exactly equal to the difference of potential energies of the two electronic states. For the PESs parametrized as in Chapter 5, this resonant absorption energy is $\hbar\omega_L^{res} = 1.90 \times 10^{-1}$ au, or 5.16 eV. If the system absorbs a photon with a frequency above the resonance value, the excess of energy is expected to be partly converted into the kinetic energy of the adsorbate as it moves on the excited PES and partly dissipated into the substrate This section presents and discusses the results of the dynamics of the desorbing species depending upon the absorbed photon frequency shift $\Delta\omega = \omega_L - \omega_L^{res}$

Figure 7.2 shows the expectation value of the adsorbate substrate distance $\langle R \rangle_t = \langle \psi^p(t)|\hat{R}|\psi^p(t)\rangle / \langle \psi^p(t)|\psi^p(t)\rangle$ as a function of time for four different frequencies of the absorbed light. The initial conditions were as discussed in Chapter 6 for excitation by a light pulse As expected the asymptotic velocity of the adsorbate increases with the frequency shift $\Delta\omega$, it is possible to estimate it directly from the graph, and therefrom calculate the kinetic energy of the adsorbate relative to the substrate Comparing the shift in the kinetic energy $\Delta E_k = E_K(\omega_L) - E_K(\omega_L^{res})$ with the frequency shift gives information about the fraction of the incident photon energy that is transferred to the relative motion of the desorbing species. The results given in the table 7.II show that, although ΔE_K increases monotonously with $\Delta\omega$ the increments are not equal nor do they change at the same rate. The reason is that a change in the absorption frequency and a consequent change in the kinetic energy deform the primary nuclear wavefunction and the energy dissipation in the substrate is altered as well This is apparent from the short time behaviour of the average R — as $\Delta\omega$ increases it appears to decrease for short time as some components of the wavepacket acquire negative values of the relative momentum later they rebound off the potential barrier of the desorbing state and the wavefunction moves toward large R faster

Table 7.II Change in the CO kinetic energy as a function of the incident photon energy

$\Delta\omega$ (eV)	E_K (eV)	ΔE_K (eV)
0.00	0.434	0.0
0.20	0.519	0.085
0.50	0.560	0.126
1.00	0.572	0.138

Figure 7.3 shows the absolute value square of the autocorrelation function followed by the plot of its natural logarithm, given by figure 7.4. It is apparent that the autocorrelation function decays more slowly at short times if the absorption frequency is increased, which can again be attributed to the deformation of the wavefunction due to the increasing kinetic energy. Figure 7.4 shows that the late time behaviour of the autocorrelation function does not change significantly within the range through which the absorption frequency was varied in the calculations. The desorption lifetime can then be deduced from the eqn. (7.2): it is approximately equal to 0.16 picoseconds for the case of resonant absorption.

Having used initial conditions for excitation by a steady light beam, figure 7.5 shows the absolute value square of the dipole dipole TCF for the Ni(001)(ads)CO system for the varying frequency of incident light; the transition dipole moment parametrization from Chapter 5 was used in the construction of the initial dipole amplitude. It is evident that the increase in the absorbed photon frequency causes broadening and a stronger pronunciation of the structure in the dipole dipole TCF. The desorption lineshape is obtained, as shown in Chapter 2, as a Fourier transform over time of the dipole-dipole TCF; the results for different photon frequencies are shown in figure 7.6.

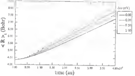

Figure 7 2 Average adsorbate substrate distance R vs time for different values of the absorbed photon frequency $\Delta\omega$ is the shift from the resonant absorption frequency

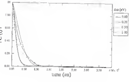

Figure 7.3 Absolute value square of the autocorrelation function vs time for different values of the absorbed photon frequency

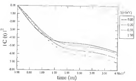

Figure 7.4 Natural logarithm of the absolute value square of the autocorrelation function vs. time for different values of the absorbed photon frequency

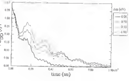

Figure 7.5 Absolute value square of the dipole-dipole time correlation function vs. time for different values of the absorbed photon frequency

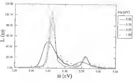

Figure 7.6 Photodesorption lineshape vs. frequency for different values of the absorbed photon frequency

The lineshape shows a peak at a frequency close to the frequency of the absorbed light, and the position of the peak changes in agreement with the absorption frequency increase, though always remaining somewhat lower. There are two reasons for this: the presence of the dissipation and the parametrization of the PESs itself — the excitation energy was not adjusted to the experimental value and the calculated value was retained instead. There is a well detectable secondary maximum in the lineshape, approximately 1 eV above the peak frequency; it is attributable to the internal vibrational excitations in the adsorbate.

Calculations of CO Photodesorption Varying the Dissipation Strength

Developing the physical model of photodesorption, it was shown in Chapter 3 that the magnitude of the dissipative imaginary potentials is directly related to both the pair correlation functions of the lattice displacements and of the electronic charge density in the substrate. However, the detailed dynamics of the metal substrate is beyond the scope of this study, so the dissipative potentials were parametrized semiempirically as the imaginary parts of the diabatic PESs and their coupling (cf. Chapter 5). They were chosen to be decaying exponential functions (for diagonal terms in the electronic basis), and a switching function (for the diabatic coupling term), with the same inverse range parameters as the corresponding potential energy functions. The magnitudes of the dissipation potentials and coupling could not be determined by the electronic structure calculations; the model calculations from the beginning of this Chapter have provided only a qualitative insight to those magnitudes, by comparison with the known lifetimes of vibrationally excited states of the adsorbate. This section presents the results of the CO photodesorption dynamics as they depend on the magnitude of the dissipative potentials and their coupling. The corresponding parameters W_g^a, W_e^a and W_e^0 were varied from the values coming from the model calculations to values 2, 4 and 10 times larger.

First, the time dependence of the expectation values for the primary coordinates R and r is shown for different values of the dissipation parameters on figures 7.7 and 7.8, respectively. The qualitative behaviour of both coordinates shows up as expected — increasing the dissipation strength lowers the asymptotic velocity of the desorbing species and also reduces the amplitude of its internal vibration. To examine more precisely the dependance of the dynamics upon the dissipation strength, one can calculate, according to the classical correspondence, the kinetic energy of the desorbing species

$$E_k = \frac{M_{CO}}{2}\left[\frac{d\langle R\rangle_t}{dt}\right]^2_{t\to\infty} \tag{7.3}$$

and also its internal vibrational energy

$$E_v = \frac{\mu_{CO}\Omega_e}{2}\left[\langle r\rangle^2_{max}\right]_{t\to\infty} - \hbar\Omega_e/2 \tag{7.4}$$

where $\langle r\rangle_{max}$ denotes the maximum displacement in r from its equilibrium position. It must be noted here that the classical result for the vibrational energy cannot be expected to give an accurate result as it does not account for the zero point energy, still, it can illustrate the effect of dissipation qualitatively. The results for E_K and E_v are summarized in table 7.III, they show that the reduction in the kinetic and the internal vibrational energy of the adsorbate is approximately proportional to the increase in the dissipation strength.

Table 7.III Kinetic and internal vibrational energy of desorbing CO as a function of the dissipation strength parameters

Dissip strength	E_K (eV)	$-\Delta E_K$ (eV)	E_v (eV)	$-\Delta E_v$ (eV)
W^0	0.536	0.0	0.352	0.0
$2\ W^0$	0.463	0.073	0.259	0.093
$4\ W^0$	0.346	0.190	0.166	0.186
$10\ W^0$	0.220	0.316	0.035	0.317

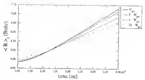

Figure 7.7. Expectation value of the adsorbate substrate distance R vs time for varying dissipation strength

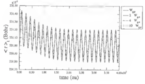

Figure 7.8 Expectation value of the C-O distance r vs. time for varying dissipation strength.

Analysis of the energy dissipation effects on the photodesorption process continues by estimating the lifetime of desorbing states for different values of the dissipation strength parameters. As before, the lifetime is deduced from the asymptotic slope of the logarithm of the absolute value square of the autocorrelation function which is shown in figure 7.9 for the dissipation strength parameters indicated before. The results for the photodesorption lifetime are given in table 7.IV; they clearly show that the desorption lifetime is inverse proportional to the dissipation strength, as in the model calculations at the beginning of the Chapter.

Table 7.IV. Photodesorption lifetime as a function of the dissipation strength, after a resonant absorption of light.

Dissipation strength parameters	Lifetime τ (ps)
W^0	0.160
2 W^0	0.086
4 W^0	0.043
10 W^0	0.019

It is also of interest to examine the effects of the energy dissipation in the substrate on a desorbing species that had initially been in a stationary state, after an electronic transition caused by a stationary light beam at the resonant absorption frequency. To this effect, the dipole-dipole TCF (figure 7.10) and the desorption lineshape (figure 7.11) were calculated for each set of the dissipation strength parameters.

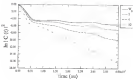

Figure 7.9: Natural logarithm of the absolute value square of the autocorrelation function vs. time for different values of the dissipation strength parameters

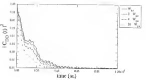

Figure 7.10 Absolute value square of the dipole-dipole TCF vs. time for different values of the dissipation strength after a resonant absorption of light.

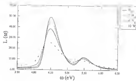

Figure 7.11 Photodesorption lineshape vs. frequency for different values of the dissipation strength after a resonant absorption of light

As could be expected, the increase in the dissipation strength causes a faster attenuation of the dipole-dipole TCF over time. As a consequence, the lineshape's largest peak, obtained from the Fourier transform of the TCF, broadens. It is also notable that the relative intensity of the secondary maximum increases, which means that the stronger dissipative coupling to the substrate causes a stronger internal vibrational excitation in the adsorbate.

The dissipative coupling between the electronic states of the adsorbate-substrate complex accounts for the possibility of electronic transitions between the two electronic basis states — those transitions are mainly the deexcitation of the Ni substrate from the 4p empty band states to the 3d/4s conduction band states. Their occurrence is manifested as the relative population of the ground electronic state, defined as

$$P_g(t) = \langle\psi_g^p(t)|\psi_g^p(t)\rangle / \left[\langle\psi_g^p(t)|\psi_g^p(t)\rangle + \langle\psi_e^p(t)|\psi_e^p(t)\rangle\right] \qquad (7.5)$$

This relative population is shown in figure 7.12 for the varying dissipation strength parameters. The results show that in all cases an electronic transition to the ground state PES is more probable and will occur at shorter times: when the dissipative coupling is increased, the short time deexcitation is more pronounced, but it disappears sooner at long times. It is apparent from figure 7.12 that the maximal probability of the electronic deexcitation increases linearly with the dissipative coupling strength.

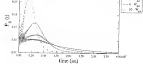

Figure 7.12 Relative population on the ground state PES vs time, for varying dissipation strength

Calculations of CO Photodesorption: Varying the Asymptotic Energy Difference between PESs

In this study's model of the CO photodesorption from nickel, the product states consist of the ground electronic state of the desorbing CO with an internal vibrational distribution, and a 4p or a 3d/4s Ni electronic band state. The energy difference between the corresponding PESs at large adsorbate-substrate distances then represents the energy difference between the two metal bands; the value of $\Delta E = 3.48$ eV was obtained by extrapolating the results of the NiCO molecule's electronic structure calculations to large R with an exponentially decaying function for the excited state PES, and it coincides with the energy difference between the Fermi level and the maximum of the 4p band density of states [Nagel 1973] for solid nickel. However, since electronic band states form an energy continuum, the asymptotic energy value on the excited state PES cannot be fixed with certainty. Therefore, the parameter ΔE of the potential energy function $V_e(R,r)$ (cf. Chapter 5) was changed in the calculations by adding a long range correction of the form

$$V_e^{corr}(R,r) = V_e(R,r) - V_{asy}^0\{1 + \tanh[\alpha_e(R - 2R_e)]\}/2 \qquad (7.6)$$

which lowers the asymptotic energy difference. The calculations were repeated for $\Delta E = 2.98$ eV, and both the autocorrelation and the dipole-dipole TCF were virtually unchanged; thus the 0.5 eV decrease in the asymptotic energy difference was not found to affect with any significance the photodesorption lifetime and lineshape. The only change was shown by the late time behaviour of the expectation value of R, illustrated by figure 7.13; however, the calculated increase in the final kinetic energy of the desorbing species is only [illegible] eV or 11% of the change in ΔE

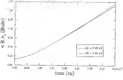

Figure 7.13 Average adsorbate-substrate distance R vs time varying the asymptotic energy difference ΔE.

CHAPTER 8
CONCLUSIONS

Contributions to the Theory of Photodesorption

The physical model developed in this dissertation describes the desorption induced by an electronic transition (DIET), caused by an interaction of UV light with a localized region of the adsorbate-substrate complex. This establishes a hierarchy of the degrees of freedom (DFs) in the complex: those that involve the operator of the transition into a desorbing state are the primary DFs and they describe the relative motion of the desorbing species with respect to the substrate as well as its internal motion, others are the secondary DFs and they describe the substrate dynamics. Primary and secondary DFs are coupled self-consistently, which leads to the energy fluctuation and dissipation in the primary DF Hamiltonian of the desorbing species. Assuming a stochastic character for the secondary DF dynamics, the energy fluctuations vanish on the average and the dissipation occurs through relaxation into a temporary equilibrium of the secondary DFs, corresponding to a time dependent temperature of the substrate.

The energy dissipation term appears in the primary DF Hamiltonian as an anti-Hermitian addition to the potential energy function, resembling the imaginary optical potentials from scattering theory. Its form was derived for two types of substrate excitations: lattice vibrations — phonons and electron hole pair excitations. In both cases, the form of the dissipative potential depends upon a time correlation function (TCF) of a substrate property. For phonons the magnitude of dissipation is proportional to the TCF of the lattice displacements while for the electronic excitations it is proportional to the charge density fluctuation TCF The self-consistent field (SCF) coupling of the primary and secondary DFs is crucial to the dissipative potential as both the displacement and the charge density fluctuation TCFs vanish in its absence. therefore the energy dissipation in the desorbing species dynamics is a direct consequence of the SCF treatment of the system that was developed in this work

The experimental conditions of photodesorption with electronic transitions may involve either the adsorbate interacting with a short pulse of light inducing an approximately instantaneous transition to the desorbing state or a steady beam of light preparing a stationary initial state for desorption. In the former case it is appropriate to measure the lifetime of the desorbing quantum state after the transition in the latter case it is possible to define the photodesorption lineshape as a function of the given light frequency The desorption lifetime can be estimated from the late time decay of the autocorrelation function — the projection of the desorption complex molecular wavefunction on its initial value The lineshape is obtained as a temporal Fourier transform of the TCF for the transition dipole moment between the electronic states of the adsorbate-substrate complex

The desorption lineshape expression in terms of the dipole-dipole TCF is analogous to the rate constant given as the integrated collisional TCF in scattering theory which was derived from the Fermi golden rule for the transition probability However the total energy in the primary DFs of the adsorbate substrate complex is not conserved in this theory due to the dissipation as a consequence the transition probability as well as the desorption lineshape, acquire a finite width and were demonstrated to become Lorentzian functions in energy with the peak shifted by the frequency of the absorbed light and the width proportional to the expectation value of the dissipative Hamiltonian. With this generalization, the concept of desorption lineshape becomes applicable to the systems including the energy dissipation.

Computational Algorithm for the CO Photodesorption from the Ni(001) Surface

The CO photodesorption dynamics was studied by solving the time dependent Schrödinger equation (TDSE) with the effective Hamiltonian of the primary DFs of the system. The desorption was modelled as a two electronic states process, with the system evolving in two primary DFs. The two electronic states were described by two complex potential energy surfaces (PESs) so the effects of the energy dissipation in the substrate were included. The PESs and their couplings were parametrized semiempirically using the available experimental data for the Ni(001)(ads)CO system and electronic structure calculations for CO bonded to a single Ni atom and an Ni_{10} cluster.

The primary TDSE was solved by propagation of wavepackets using the split operator propagation scheme to construct the time evolution operator with a modification to include the imaginary dissipative potentials. The diabatic electronic representation was used in the time propagation because it eliminates momentum couplings between the electronic basis states; the real and imaginary potential energy matrices were diagonalized separately by orthogonal transformations. The time propagation algorithm was implemented numerically using a discrete grid to represent the coordinate and momentum space — the variables of each factor in the split operator propagator were chosen such that the Hamiltonian in each factor was diagonal, and the coordinate and momentum space were related by a Fourier transformation. A fast Fourier transform (FFT) algorithm was employed to construct the kinetic energy propagator.

Summary of Results of the CO Photodesorption Calculations

The calculations of the CO photodesorption in this study were done varying three different parameters: the frequency of the absorbed light (starting with a resonant absorption), the magnitude of the dissipative imaginary potentials and their coupling, and the asymptotic energy difference between the two primary electronic states. The dependence on the incoming photon frequency is important because the exact resonance absorption frequency, in this case corresponding to a wavelength of 240 nm, may not be experimentally available. The magnitudes of dissipation potentials and their coupling were varied, as they had been left as free parameters in the construction of the model: neither previous references nor the electronic structure calculations could provide their values. Finally the asymptotic energy difference was varied because the electronic basis states in the model represent the CO molecular orbitals coupled with the Ni band orbitals, so a continuous variation of the energy difference between those states is possible.

The photodesorption lineshape for the case of resonant absorption (fig. 7.6, solid line) shows two peaks between 4.25 eV and 5.75 eV; the largest peak is centered at the energy of 4.50 eV with a half width of 0.50 eV. This is comparable with the EELS spectroscopy result [Akimoto et al. 1979] that shows a peak at 5.8

eV with a half width of approximately 1 eV. This means that the semiempirical parametrization for the PESs and their couplings used in the calculations gives a good qualitative description of the Ni(001)(ads)CO system, even though the potential energy functions were obtained with a single Ni atom or a relatively small 10-atom cluster simulating the solid nickel.

The results for the logarithm of the square modulus of the autocorrelation function varying the absorbed photon frequency (fig. 7.4) and the dissipation strength parameters (fig. 7.9) show that the decay of the desorbing state is not exponential at short times. This is evidence that the electronic transitions in the adsorbate-substrate complex occur both through the diabatic coupling of the PESs and through the dissipative coupling that represents the primary DF deexcitation via the energy dissipation in the substrate. These transitions are evident in the results for the relative population of the ground electronic state of the complex (fig. 7.12): it is clear that their probability is proportional to the dissipative coupling strength; even in the absence of dissipation there is a finite probability to find the system in its ground electronic state due to the diabatic coupling at short adsorbate-substrate distance.

From the expectation value over time for the adsorbate-substrate distance R (figs. 7.2 and 7.7) it is possible to calculate the kinetic energy of the desorbing CO molecule and examine its dependence on the absorbed light frequency and the dissipation strength. If the frequency of the absorbed photon is above the resonance, the additional photon energy becomes the kinetic energy of the initial state of propagation, with a momentum distribution that averages out to zero (because of the assumed Franck-Condon electronic transition upon absorption). As a consequence, the corresponding wavepacket is expected to deform at short times and later evolve in the asymptotic region of large R with a larger velocity. The results (fig. 7.2) showed this behaviour, as the wavepacket initially spends a longer time in the region close to the adsorption site to later move away from it faster. However, not all of the extra energy from the light absorption is converted to the asymptotic kinetic energy (table 7.II), due to the presence of dissipative potentials. When the dissipation strength is increased, both the relative kinetic energy and the internal vibrational energy of the desorbing species are reduced (figs. 7.7 and 7.8, table 7.III).

From the results of the square modulus of the autocorrelation function (figs. 7.4 and 7.9), it is apparent that the desorption lifetime evaluated from the exponential decay of the autocorrelation function at late times bears no significant dependence on the absorbed photon frequency, at least within the interval of the calculations; however, it is clearly inverse proportional to the dissipation strength (table 7.IV), which is the same dependence that had been observed in the model calculations in Chapter 7. These results mean that the energy of absorbed light is distributed quickly (within the time at which the adsorbed molecule is still close to the substrate) and, except for a small change in the kinetic energy of the desorbing species, it does not significantly affect the late time dynamics. On the other hand, the energy dissipation in the substrate plays a crucial role in the photodesorption dynamics, both for the lifetime of desorbing states and for the internal vibrations of the desorbing species (fig. 7.8).

Outlook for Future Research

This study has developed a theory of photodesorption that includes the continuous energy spectrum of the substrate through the SCF coupling, and directly incorporates the energy dissipation in the substrate into the quantum dynamics of the desorbing species. It has been shown that the magnitude of dissipation is related to the TCFs of the lattice displacements and the electronic density fluctuations in the substrate metal, and the computational results show that it significantly influences the motion of the adsorbate. The next step should be a detailed study of the nature of the adsorbate-substrate coupling which should give exact results for the dissipative potentials and couplings to substitute their semiempirical parametrization in this work. Also, the theory would benefit from higher quality *ab initio* calculations of the excited electronic state PES to improve its parametrization and reproduce more closely the experimental results.

A numerical algorithm for the wavepacket propagation in two degrees of freedom over two coupled complex PESs was developed and applied on the case of CO desorbing from the Ni(001) surface. It allows for a quantum mechanical calculation of the adsorbate's motion relative to the substrate and its internal vibration. However, the rotational motion of the desorbing species is not taken into account, so a further improvement of the algorithm would have to include another degree of freedom — a rotation angle of the diatomic. A practical obstacle in this development is the fact that the computational time and effort increases approximately quadratically with the number of discrete grid points per each degree of freedom, so it may be necessary to employ more economical numerical methods, such as the discrete variable representation (DVR) [Light et al 1985] Also, the presence of a continuum of substrate electronic states may imply that there may be more than one excited electronic state of the adsorbate-substrate complex involved in the dynamics, so the algorithm should be modified to include another PES coupled diabatically to the existing ones. This would obviously increase the size of matrices involved in the computation and also make the transformation between the electronic representations more complicated, although conceptually unchanged

Finally, it can be expected that recent developments in sub-picosecond laser spectroscopy should produce more high quality results of time resolved experiments on the molecules adsorbed on metal surfaces. This should provide more information to further improve the parametrization of model potentials and couplings

APPENDIX A

RATE CONSTANT IN TERMS OF A COLLISIONAL TIME CORRELATION FUNCTION FOR A DISSIPATIVE SYSTEM

This appendix contains a detailed derivation for the reaction rate constant expressed as a time integral of a collisional time correlation function (TCF) for a dissipative system interacting with an external radiation field. It is a generalization of the previous work [Micha 1981; Micha and Vilallonga 1985] to take into account the energy dissipation in the present system, in the case of interest, it comes from the coupling of the CO adsorbate to an energy continuum of the infinite Ni substrate, and as a consequence the effective Hamiltonian for the region around the adsorbate contains an imaginary term and is not a Hermitian operator.

One starts by separating the system-radiation term from the rest of the primary effective Hamiltonian

$$\hat{F}_p = \hat{F}_0 + H_{pL}$$
$$\hat{F}_0 = \hat{H}_p + \hat{H}_L - iW_p/2 \qquad \text{(A 1)}$$

where all the operators have been defined in Chapter 2. This is similar to the standard separation of perturbation theory, but in this case there are in principle no limits to the coupling strength. The "uncoupled" Hamiltonian $\hat{F}_0$ is obviously not Hermitian, so it defines a "right" eigenvalue problem

$$\hat{F}_0|\phi_n^0\rangle = (E_n - iW_n/2)|\phi_n^0\rangle \qquad \text{(A 2)}$$

and a "left" eigenvalue problem

$$\hat{F}_0^\dagger|\tilde{\phi}_n^0\rangle = (E_n + iW_n/2)|\tilde{\phi}_n^0\rangle \qquad \text{(A 3)}$$

where the complex eigenvalues are determined by $E_n = \langle\tilde{\phi}_n^0|(\hat{H}_p + \hat{H}_L)|\phi_n^0\rangle/\langle\tilde{\phi}_n^0|\phi_n^0\rangle$ and $W_n = \langle\tilde{\phi}_n^0|W_p|\phi_n^0\rangle/\langle\tilde{\phi}_n^0|\phi_n^0\rangle$. The left and right eigenvectors combine for the orthonormality and closure relations as follows

$$\begin{aligned} \langle\tilde{\phi}_n^0|\phi_m^0\rangle &= \delta_{n,m} \\ \sum_m |\phi_m^0\rangle\langle\tilde{\phi}_m^0| &= \hat{I} \end{aligned} \tag{A.4}$$

From eqns. (A.2) and (A.3), it follows that the time evolution operator with $\hat{F}_0$ acts on the right and left eigenvectors producing

$$\begin{aligned} \exp\left(-i\hat{F}_0 t/\hbar\right)|\phi_n^0\rangle &= |\phi_n^0\rangle \exp[-i(E_n - iW_n/2)t/\hbar] \\ \langle\tilde{\phi}_n^0|\exp\left(i\hat{F}_0 t/\hbar\right) &= \exp[i(E_n - iW_n/2)t/\hbar]\langle\tilde{\phi}_n^0| \end{aligned} \tag{A.5}$$

In analogy with Chapter 2, the partitioning (A.1) of the effective Hamiltonian defines an interaction picture in which

$$\begin{aligned} |\psi^p(t)\rangle_I &= \exp\left(i\hat{F}_0 t/\hbar\right)|\psi^p(t)\rangle \\ \hat{F}_I(t) &= \exp\left(i\hat{F}_0 t/\hbar\right)\hat{H}_{pL}\exp\left(-i\hat{F}_0 t/\hbar\right) \end{aligned} \tag{A.6}$$

so the primary TDSE becomes

$$i\hbar\frac{\partial}{\partial t}|\psi^p(t)\rangle_I = \hat{F}_I(t)|\psi^p(t)\rangle_I \tag{A.7}$$

This equation can be integrated formally to obtain

$$|\psi^p(t)\rangle_I = |\psi^p(0)\rangle_I - \frac{i}{\hbar}\int_0^t F_I(t')|\psi^p(t')\rangle_I\, dt' \tag{A.8}$$

From the definition of the interaction picture $|\psi^p(0)\rangle_I = |\psi^p(0)\rangle$, and in the lowest order of iteration, the interaction picture solution becomes

$$|\psi^p(t)\rangle_I = \left[I - \frac{i}{\hbar}\int_0^t F_I(t')dt'\right]|\psi^p(0)\rangle \tag{A.9}$$

For a particular choice of initial conditions $|\psi^p(0)\rangle = |\phi_n^0\rangle$ this becomes

$$|\psi_n^p(t)\rangle_I = \left[I - \frac{i}{\hbar}\int_0^t F_I(t')dt' \right]|\phi_n^0\rangle \tag{A.10}$$

In analogy with the case of a Hermitian Hamiltonian one defines a state to state rate constant [Rodberg and Thaler 1967] as

$$R_{m\to n} = \frac{d}{dt}\left|\langle\bar{\phi}_n^0|\psi_{I(m)}^p(t)\rangle\right|^2 = \frac{d}{dt}|A_{m\to n}(t)|^2 \tag{A.11}$$

where $A_{m\to n}(t)$ denotes a projection of the interaction picture wavefunction (A.10) onto the left eigenstate $|\bar{\phi}_n^0\rangle$ of $\hat{F}_0$. Inserting (A.10) into the equation for $A_{m\to n}(t)$ using the time dependence (A.6) of $\hat{F}_I$ and relations (A.5) to operate on the eigenstates, and finally integrating over time the projection $A_{m\to n}(t)$ becomes

$$A_{m\to n}(t) = \delta_{mn} + \frac{\langle\bar{\phi}_n^0|H_{pL}|\phi_m^0\rangle\left\{e^{-i[(E_m-E_n)-i(W_m-W_n)/2]t/\hbar} - 1\right\}}{(E_m-E_n)^2+(W_m-W_n)^2/4} \tag{A.12}$$

where the delta function comes from the orthonormality (A.4). Inserting (A.12) into (A.11) yields the state to state rate constant

$$R_{m\to n} = \frac{1}{\hbar}\left|\langle\bar{\phi}_n^0|H_{pL}|\phi_m^0\rangle\right|^2\frac{(W_m-W_n)}{(E_m-E_n)^2+(W_m-W_n)^2/4} \tag{A.13}$$

It is noteworthy that in the absence of dissipation, i.e. in the limit of W_m and W_n both going to zero, the Lorentzian in (A.13) becomes a Dirac delta function in energy, thus recovering the known Fermi golden rule result [Rodberg and Thaler 1967, Schiff 1968].

To convert the rate constant (A.13) into an integral of a TCF the Lorentzian in energy must be expressed as

$$\frac{(W_m-W_n)}{(E_m-E_n)^2+(W_m-W_n)^2/4} = \frac{2}{\hbar}Re\int_0^\infty e^{-i[(E_m-E_n)-i(W_m-W_n)/2]t/\hbar}dt \tag{A.14}$$

and then inserted into (A.13). Splitting up the absolute value square of the $\hat{H}_{pl}$ matrix element using again relations (A.5) for the time evolution of the $\hat{F}_0$ eigenstates, averaging over the initial states with index n and summing over the final states with index m the cumulative rate constant becomes

$$R = \frac{2}{\hbar^2} Re \sum_m w_m \int_0^\infty \langle\phi_m^0|F_I^\dagger(0)\left[\sum_n |\bar\phi_n^0\rangle\langle\tilde\phi_n^0|\right] F_I(t)|\phi_m^0\rangle dt \qquad \text{(A.15)}$$

where w_m are statistical weights of eigenstates $|\phi_m^0\rangle$. The remaining problem is the summation over n, because the square bracket in (A.15) is not equal to the identity given by the closure relation (A.4). However, from (A.2) and (A.3) it follows that any left eigenstate can be expressed in terms of the corresponding right eigenstate as

$$\begin{aligned} |\tilde\phi_n^0\rangle &= \left(I + \Pi\right)|\phi_n^0\rangle \\ \Pi &= i\left[\left(\hat{F}_0 - E_n\hat{I}\right) - i\left(W + iW_n I/2\right)\right]^{-1}\left(W - W_n I\right) \end{aligned} \qquad \text{(A.16)}$$

For a relatively weak dissipation, the operator Π can be neglected, so the left eigenvalue $|\tilde\phi_n^0\rangle$ in (A.15) can be substituted by its right counterpart, after which the summation over n gives an identity and the cumulative rate constant becomes an integral of a collisional TCF [Micha 1981, Micha and Vilallonga 1985]

$$R = \frac{2}{\hbar^2} Re \int_0^t \langle\langle \hat{F}_I^\dagger(t) F_I(0)\rangle\rangle \, dt \qquad \text{(A.17)}$$

where the system-field coupling Hamiltonian is identified as a transition operator and $\langle\langle\ \ \rangle\rangle$ denotes a statistical average over the initial distribution $\{w_m\}$.

APPENDIX B

INPUT DATA FOR THE ZINDO CALCULATIONS OF NiCO and $Ni_{10}CO$

This appendix contains information on the input data for the ZINDO calculations that were done on the $Ni_{10}CO$ and NiCO systems

Specifying the atomic positions for CO adsorbed on a Ni_{10} cluster it was taken into account that metal nickel forms a BCC crystal lattice the cluster was constructed from the first and second nearest neighbours of the adsorption site Ni atom, and an additional atom directly below the adsorption site The atomic Cartesian coordinates (in Angströms) are given in table B 1

Table B 1 Atomic coordinates for CO adsorbed on a Ni_{10} cluster

Atom	x	y	z
O	0.00	0.00	varied
C	0.00	0.00	varied
Ni (ads site)	0.00	0.00	0.00
Ni	1.76	1.76	0.00
Ni	1.76	-1.76	0.00
Ni	-1.76	1.76	0.00
Ni	-1.76	-1.76	0.00
Ni	1.76	0.00	-1.76
Ni	0.00	1.76	-1.76
Ni	-1.76	0.00	-1.76
Ni	0.00	-1.76	1.76
Ni	0.00	0.00	3.54

The remainder of this appendix discusses other relevant parameters for the ZINDO calculations The SCF basis set for the ground electronic state energy calculation is specified according to the atoms in the system, in this case it consists of two atoms with s and p orbitals (O and C) and one (or 10) atoms with s p and d orbitals for each of the Ni atoms. The important distinction is made in the treatment of two-electron integrals in the Hartree Fock SCF calculations for the ground state energy one must use their theoretical parameters (theoretical gammas), whereas in the CI calculations of the excited states the parameters that are used come from spectroscopy (spectroscopical gammas). Other important parameters are listed in table B II below

Table B II. Input parameters for the ZINDO calculations of NiCO and $Ni_{10}CO$

System	NiCO	$Ni_{10}CO$
Total no. of valence electrons	20	110
Spin multiplicity in SCF	1	3
No. of open shells in ROHF/SCF	/	2
No. of configurations in CI	80	110

APPENDIX C
FLOW CHART OF THE COMPUTER PROGRAM FOR TIME EVOLUTION OVER TWO COMPLEX PESs IN TWO DEGREES OF FREEDOM

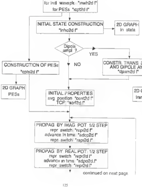

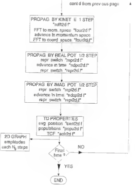
cont'd from previous page
PROPAG BY KINET E 1 STEP
"adft2d f"
FFT to mom. space "four2d f"
advance in momentum space
FFT to coord space "four2d f"
PROPAG BY REAL POT 1/2 STEP
repr switch "repr2d f"
advance in time "adpo2d f"
repr switch "repr2d f"
PROPAG BY IMAG POT 1/2 STEP
repr switch "repi2d f"
advance in time "adop2d f"
repr switch "repi2d f"
TD PROPERTIES
avg position "cent2d f
populations "popu2d f"
TCF "acfr2d f"
2D GRAPH
amplitudes
each N_g steps
Final time ?
NO
YES
END

BIBLIOGRAPHY

Adelman S. A. and J. D. Doll, Acc. Chem. Res. **10**, 378 (1977)

Akimoto K., Y. Sakisaka, M. Nishijima and M. Onchi, Surf. Sci. **88**, 109 (1979)

Albert M. R. and J. R. Yates, *The Surface Scientist's Guide to Organometallic Chemistry* (Am. Chem. Soc. Washington 1987), chap. 5

Alvarellos J. and H. Metiu, J. Chem. Phys. **88**, 4957 (1988)

Andersson S. and J. B. Pendry, Phys. Rev. Lett. **43**, 363 (1979)

Arfken G., *Mathematical Methods for Physicists* (Academic Press, New York 1985), chap. 4

Arlinghaus F. J., J. G. Gay and J. R. Smith, Phys. Rev. B **21**, 2055 (1980)

Arlinghaus F. J., J. G. Gay and J. R. Smith, in *Theory of Chemisorption*, ed. J. R. Smith (Springer Verlag, Berlin 1980), p. 71

Avouris P. and R. E. Walkup, Ann. Rev. Phys. Chem. **40**, 173 (1989)

Baer M., Chem. Phys. **15**, 49 (1979)

Baer M., in *Theory of Chemical Reaction Dynamics*, ed. M. Baer (CRC Press, Boca Raton 1985), vol. II, chap. 4

Bekšić D. and D. A. Micha, to be published

Bekšić D., J. D. da Motta Neto and D. A. Micha, to be published

Berne B. J., *Physical Chemistry: an Advanced Treatise*, ed. D. Henderson (Academic Press, New York 1971), vol. 8B

Berne B. J. and D. Forster, Ann. Rev. Phys. Chem. **22**, 563 (1971)

Betz G. and P. Vargas, eds., *Desorption Induced by Electronic Transitions DIET IV* (Springer Verlag, Berlin 1990)

Bittner E. R. and J. C. Light, J. Chem. Phys. **99**, 8237 (1993)

Black J. E., D. A. Campbell and R. F. Wallis, Surf. Sci. **105**, 629 (1981)

Black J. E., P. Bopp, K. Lutzenkirchen and M. Wolfsberg, J. Chem. Phys. **85**, 6431 (1982)

Blum K., *Density Matrix Theory and Applications* (Plenum Press, New York 1981), chap. 7

Blyholder G., Surf. Sci. **42**, 249 (1974)

Brako R. and D. M. Newns, J. Phys. C **14**, 3065 (1981)

Brako R. and D. M. Newns, Rep. Prog. Phys. **52**, 655 (1989)

Brenig W., Z. Physik B **23**, 361 (1976)

Brenig W., J. Phys. Soc. Japan **51**, 1915 (1982)

Brenig W. and D. Menzel eds., *Desorption Induced by Electronic Transitions DIET II* (Springer-Verlag, Berlin 1984)

Brivio G. P. and T. B. Grimley, Surf. Sci. **89**, 226 (1979)

Bross H., G. Bohn, G. Meister, W. Schubö and H. Stöhr in *Computational Methods in Band Theory* eds. P. M. Marcus, J. F. Janak and A. R. Williams (Plenum Press, New York 1971) p. 44

Burns A. R., E. B. Stechel and D. R. Jennison eds., *Desorption Induced by Electronic Transitions DIET V* (Springer Verlag, Berlin 1993)

Campos-Martínez J. and R. D. Coalson, J. Chem. Phys. **93**, 4740 (1990)

Cavanagh R. R., D. S. King, J. C. Stephenson and T. F. Heinz, J. Phys. Chem. **97**, 786 (1993)

Cederbaum L. S. and F. Tarantelli, J. Chem. Phys. **98**, 9691 (1993)

Coalson R. D., J. Chem. Phys. **83**, 688 (1985)

Coalson R D., Adv Chem Phys **73** 605 (1989)

Cohen J M and D A. Micha, J Chem Phys **97,** 1038 (1992)

Colbert D T and W H Miller J Chem Phys **96** 1982 (1992)

Cortes E B J West and K Lindenberg J Chem Phys **82**, 2708 (1985)

Drakova D and G Doyen Surf Sci **226**, 263 (1990)

Ehrenreich H. and M H Cohen Phys Rev **115** 786 (1959)

Feit M D , J A. Fleck and A Steiger, J Comp Phys **47** 412 (1982)

Fernández F M and D A Micha, J Chem Phys. **98** 8173 (1992)

Ford G. W , J. T Lewis and R. F O'Connell, Phys Rev A **37,** 4419 (1988)

Gadzuk J W in *Vibrational Spectroscopy of Molecules and Surfaces* eds T Yates and T E Madey (Plenum Press, New York 1987) p 49

Gadzuk J W Ann Rev Phys Chem **39**, 395 (1988)

Gadzuk J. W , Phys Rev **B44** 13466 (1991)

Gadzuk J W , L J Richter S A Buntin, D S King and R. R Cavanagh Surf Sci **235** 317 (1990)

Gerber R B V Buch and M Ratner, J Chem Phys **77,** 3022 (1982)

Germer T A , J C Stephenson E J Heilweil and R. R. Cavanagh J Chem Phys **98** 9886 (1993)

Germer T A , J C Stephenson, E. J Heilweil and R R Cavanagh J Chem Phys **101** 1 (1994)

Grimley T B Proc Phys Soc London **90,** 751 (1967)

Hamilton I P and J C. Light J Chem Phys **84**, 306 (1986)

Hammerich A D R Kosloff and M. A. Ratner Chem Phys Lett. **171,** 97 (1990)

Head-Gordon M. and J. C. Tully, J. Chem. Phys. **96**, 3939 (1992)

Head-Gordon M. and J. C. Tully, Phys. Rev. B**46**, 1853 (1992)

Heather R. and H. Metiu, J. Chem. Phys. **86**, 5009 (1987)

Hermann K. and P. D. Bagus, Phys. Rev. B **16**, 4195 (1977)

Herzberg G., *Spectra of Diatomic Molecules* (Van Nostrand, New York 1960)

Heskett D., I. Strathy, E. W. Plummer and R. A. de Paola, Phys. Rev. B **32**, 6222 (1985)

Hoffmann R., *Solids and Surfaces — A Chemist's Point of View* (VCH Publ., New York 1988)

Hynes J. T. and J. M. Deutch in *Physical Chemistry, an Advanced Treatise* vol. 11B, eds. E. Eyring, W. Jost and D. Henderson (Academic Press, New York 1975), p. 729

Jackson B., J. Chem. Phys. **88**, 1384 (1988)

Jackson B., J. Chem. Phys. **90**, 140 (1989)

Jackson J. D., *Classical Electrodynamics* (John Wiley, New York 1975), chap. 4

Kampen N. G. van, *Stochastic Processes in Physics and Chemistry* (North Holland, Amsterdam 1981), chap. 8

King D. S. and R. R. Cavanagh, Adv. Chem. Phys. **76**, 45 (1989)

Kittel C., *Quantum Theory of Solids* (John Wiley, New York 1963), chaps. 5, 6

Kotler Z., A. Nitzan and R. Kosloff, Chem. Phys. Lett. **153**, 483 (1988)

Kubo R., M. Toda and N. Hashitsume, *Statistical Physics II*, 2nd ed. (Springer Verlag, Berlin 1991), chap. 2

Kumamoto D and R Silbey J Chem Phys **75** 3035 (1982)

Lanczos C. J. Res. Natl Bur Stand **45** 255 (1950)

Langreth D and H Suhl eds *Many Body Phenomena at Surfaces* (Academic Press, New York 1984)

Launay J de, *Solid State Physics* vol 2 F Seitz and D Turnbull eds (Academic Press, New York, 1955) p 220

Leforestier C., R Bisseling C Cerjan M D Feit R. Friesner A Guldberg A Hammerich G Jolicard, W Karrlein H D Meyer N Lipkin O Roncero and R. Kosloff J Comp. Phys **94** 59 (1991)

Light J C, I P Hamilton and J V Lill, J Chem Phys **82**, 1400 (1985)

Lin J T and T F George J Chem Phys **72** 2554 (1980)

Liu M C and G Ertl, Ann Rev Phys Chem **37** 587 (1987)

López Sancho J M and J Rubio Surf Sci **108**, L399 (1981)

Louisell W H. *Quantum Statistical Properties of Radiation* (John Wiley New York 1973)

Lovesey S W., *Condensed Matter Physics — Dynamic Correlations* (Benjamin/Cummings Reading 1980) chap 3

Magnus W Comm. Proc Appl. Math **7** 649 (1954)

Makri N and W H Miller J Chem Phys **87** 7581 (1987)

Manthe U. H-D Meyer and L. S Cederbaum, J Chem. Phys **97** 3199 (1992)

Manthe U., H-D Meyer and L. S Cederbaum J Chem Phys **97** 9062 (1992)

March N H W H Young and S Sampanthar *The Many Body Problem in Quantum Mechanics* (Cambridge Univ Press Cambridge 1967) chap 1

Marston J. B., D. R. Andersson, E. R. Behringer, B. H. Cooper, C. A. DiRubio, G. A. Kimmel and C. Richardson, Phys. Rev. B **48**, 7809 (1993)

Marucn R., T. Kusuma, V. Hicks and A. Companion, Surf. Sci. **236**, 210 (1990)

McWeeny R., *Methods of Molecular Quantum Mechanics* (ed. Academic Press, New York 1992), chap. 5

Menzel D., J. Vac. Sci. Technol. **20**, 538 (1982)

Menzel D., Ber. Bunsenges. Phys. Chem. **72**, 591 (1986)

Menzel D. and R. Gomer, J. Chem. Phys. **41**, 3311 (1964)

Messina M. and R. D. Coulson, J. Chem. Phys. **95**, 8977 (1991)

Micha D. A. in *Dynamics of Molecular Collisions* Part A, ed. W. H. Miller (Plenum Press, New York, 1976), p. 81

Micha D. A., J. Chem. Phys. **70**, 565 (1979)

Micha D. A., Chem. Phys. Lett. **81**, 517 (1981)

Micha D. A. and E. Q. Feng, Comp. Phys. Commun. **80**, 242 (1994)

Micha D. A. and Z. Parra, J. Phys. Chem. **92**, 3236 (1988)

Micha D. A. and K. Runge, *Time Dependent Quantum Molecular Dynamics*, ed. J. Broeckhove (Plenum Press, New York 1992), p. 247

Micha D. A. and D. Srivastava, Chem. Phys. Lett. **162**, 376 (1989)

Micha D. A. and E. Vilallonga, J. Chem. Phys. **84**, 3162 (1986)

Miller W. H., J. Chem. Phys. **61**, 1823 (1974)

Miller W. H. in *Stochasticity and Intramolecular Redistribution of Energy*, eds. R. Lefevbre and S. Mukamel (Reidel, Boston 1987), p. 263

Miller W H S D Schwartz and J W Tromp, J Chem Phys **79**, 4889 (1983)

Misewich J A T F Heinz and D M Newns, Phys Rev Lett. **68** 3737 (1992)

Mori H, Prog Theor Phys **33**, 423 (1965)

Nagel D J, *Band Structure and Spectroscopy of Metals and Alloys*, ed. D J Fabian and L M Watson (Academic Press, New York 1973) p 457

Newns D M, T F Heinz and J A Misewich, Prog Theor Phys Suppl **106** 411 (1991)

Norskov J K, Rep Prog. Phys. **53** 1253 (1990)

Olson J A. and D A Micha, Int. J Quantum Chem. **22**, 971 (1982)

Paldus J and J Čižek, Adv Quantum Chem **9**, 105 (1975)

Papaconstantopulous D A *Handbook of the Band Structure of Elemental Solids*, (Plenum Press, New York 1986) p 111

Parra Z. and D A Micha, Chem Phys Lett. **132**, 488 (1986)

Persson B N J, Phys Rev B **44** 3277 (1991)

Persson B N J and M Persson Solid State Commun 36 175 (1980)

Persson B N J and M Persson Surf Sci **97**, 609 (1980)

Persson B N J and R Ryberg Phys Rev B **40** 10273 (1989)

Press W H, S A Teukolsky, V T Vetterling and B P Flannery *Numerical Recipes in Fortran* (Cambridge Univ Press, Cambridge 1992) chap. 12

Prybyla J A., T F Heinz J A Misewich, M M T Loy and J H Glownia, Phys Rev Lett. **64** 1537 (1990)

Prybyla J A, H W K. Tom and G D Aumiller, Phys Rev Lett 68 503 (1992)

Redhead P. A., Can. J. Phys. **42**, 886 (1964)

Richardson A. M. and A. M. Bradshaw Surf. Sci. **88** 255 (1979)

Ridley J. E. and M. C. Zerner, Theoret. Chim. Acta **32**, 111 (1973)

Rodberg L. S. and R. M. Thaler *The Quantum Theory of Scattering* (Academic Press, New York, 1967), chap. 8

Sawada K. Phys. Rev. **106** 372 (1957)

Schiff L. I. *Quantum Mechanics* (McGraw Hill, Hong Kong 1968), chap. 9

Schuck P. and W. Brenig, Z. Phys. B **46**, 137 (1982)

Seideman T. and W. H. Miller, J. Chem. Phys. **96** 4412 (1992)

Shugard M., J. C. Tully and A. Nitzan, J. Chem. Phys. **66** 2534 (1977)

Smith F. T. Phys. Rev. **179** 111 (1969)

Srivastava D. and D. A. Micha Chem. Phys. Lett. **162**, 381 (1989)

Srivastava D. and D. A. Micha, J. Chem. Phys. **94** 4900 (1991)

Srivastava D. and D. A. Micha, J. Chem. Phys. **95** 380 (1991)

Stulen R. H. and M. L. Knotek eds. *Desorption Induced by Electronic Transitions DIET III* (Springer Verlag, Berlin 1988)

Sung S. S. and R. Hoffmann J. Am. Chem. Soc. **107** 578 (1985)

Truong T. N., J. J. Tanner P. Bala, J. A. McCammon, D. J. Kouri B. Lesying and D. K. Hoffman J. Chem. Phys. **96** 2077 (1992)

Tolk N. H., M. M. Traum, J. C. Tully and T. E. Madey, eds. *Desorption Induced by Electronic Transitions DIET I* (Springer Verlag, Berlin 1983)

Tully J. C., Phys. Rev. B **16** 4324 (1977)

Tully J. C., Ann. Rev. Phys. Chem. **31**, 319 (1980)

Tully J. C. in *Desorption Induced by Electronic Transitions DIET I* eds. N. H. Tolk, M. M. Traum, J. C. Tully and T. E. Madey (Springer Verlag, Berlin 1983)

Wilcox R. M., J. Math. Phys. **8**, 962 (1967)

Yamashita K. and W. H. Miller, J. Chem. Phys. **82**, 5475 (1985)

Zangwill A., *Physics at Surfaces* (Cambridge Univ. Press, Cambridge 1988) chap. 12

Zerner M. C., G. H. Loew, H. Kirschner and U. T. Müller Westerhoff, J. Amer. Chem. Soc. **102** 589 (1980)

Zwanzig R., *Lectures in Theoretical Physics*, vol. III, ed. W. Brittin et al. (Wiley Interscience, New York 1961), p. 106

BIOGRAPHICAL SKETCH

Dario Bekšić was born on May 31^{st} 1964 in Zagreb, Croatia, as the only child of Zorica and Vladimir. He received a solid general education at the Fifth Lyceum of his home city and proceeded toward a university degree in physics from the College of Natural Sciences and Mathematics at the University of Zagreb in 1989. His graduation thesis titled "Fermi Resonance in Molecular Vibrations" was completed at the "Rugjer Bošković Institute" in Zagreb. He came to the University of Florida in August of 1989 and started his doctoral research at the Quantum Theory Project the following year, under the prudent guidance of Dr. David A. Micha. Results of his research were presented at the international conferences Sanibel Symposia '92–'94, in Würzburg (Germany) '91, in Girona (Catalunya) '93, and in Salamanca (Spain) '94.

After completing his PhD studies at UF, Dario intends to return to his new home at Manresa (Catalunya), to enjoy many future years with his wife Neus Sitjes and his stepson Aleix, and to try to continue his professional career there.

I certify that I have read this study and that in my opinion it conforms to acceptable standards of scholarly presentation and is fully adequate, in scope and quality, as a dissertation for the degree of Doctor of Philosophy

David A. Micha Chair
Professor of Physics and
Chemistry

I certify that I have read this study and that in my opinion it conforms to acceptable standards of scholarly presentation and is fully adequate, in scope and quality, as a dissertation for the degree of Doctor of Philosophy

HJ Monkhorst

Hendrik J Monkhorst
Professor of Physics

I certify that I have read this study and that in my opinion it conforms to acceptable standards of scholarly presentation and is fully adequate, in scope and quality, as a dissertation for the degree of Doctor of Philosophy

David B Tanner
Professor of Physics

I certify that I have read this study and that in my opinion it conforms to acceptable standards of scholarly presentation and is fully adequate, in scope and quality, as a dissertation for the degree of Doctor of Philosophy

James W Dufty
Professor of Physics

I certify that I have read this study and that in my opinion it conforms to acceptable standards of scholarly presentation and is fully adequate in scope and quality, as a dissertation for the degree of Doctor of Philosophy

Philip J Brucat
Associate Professor of Chemistry

This dissertation was submitted to the Graduate Faculty of the Department of Physics in the College of Liberal Arts and Sciences and to the Graduate School and was accepted as partial fulfillment of the requirements for the degree of Doctor of Philosophy

December 1994

Dean Graduate School